2016

STRIDE | Southeastern Transportation Research, Innovation, Development and Education Center

Final Report

Infrastructure Adaptation Planning for Autonomous Vehicles

Zhibin Chen and Yafeng Yin, Ph.D., University of Florida

October 2016

TABLE OF CONTENTS

DISCLAIMER

The contents of this report reflect the views of the authors, who are responsible for the facts and the accuracy of the information presented herein. This document is disseminated under the sponsorship of the U.S. Department of Transportation's University Transportation Centers Program, in the interest of information exchange. The U.S. Government assumes no liability for the contents or use thereof.

ACKNOWLEDGMENT OF SPONSORSHIP

This work was sponsored by a grant from the Southeastern Transportation Research, Innovation, Development and Education (STRIDE) Center, a U.S. DOT Region 4 grant-funded University Transportation Center.

LIST OF AUTHORS

Zhibin Chen, University of Florida; zhibinchen@ufl.edu

Yafeng Yin, Ph.D., University of Florida; yafeng@ce.ufl.edu

LIST OF TABLES

LIST OF FIGURES

ABSTRACT

This report advocates the need for infrastructure planning to adapt to and further promote the deployment of autonomous vehicle (AV) technology. It is envisioned that in the future government agencies will dedicate certain lanes and areas of road networks to AVs only to facilitate the formulation of vehicle platoons to improve throughput and hopefully improve the performance of the whole network.

This report consists of two applications, AV lanes and AV zones. A mathematical approach is first developed to optimize a time-dependent deployment plan of AV lanes on a transportation network with heterogeneous traffic stream consisting of both conventional vehicles (CVs) and AVs, so as to minimize the social cost and promote the adoption of AVs. The deployment plan indicates when, where, and how many AV lanes to be located. The report also presents a mathematical framework for the optimal design of AV zones in a general network. With the presence of AV zones, AVs may apply different routing principles outside of and within the AV zones. A novel network equilibrium model is thus firstly proposed to capture such mixed-routing behaviors. A mixed-integer bi-level programming model is then formulated to optimize the deployment plan of AV zones. Numerical examples are presented to demonstrate the performance of the proposed models.

Keywords: autonomous vehicle; autonomous-vehicle lane; autonomous-vehicle zone; mixed routing equilibrium; market penetration; deployment plan

EXECUTIVE SUMMARY

The objectives of this project are to (a) develop a mathematical approach to optimize a time-dependent deployment plan of autonomous vehicle (AV) lanes, and (b) present a mathematical framework for the optimal design of AV zones in a general network.

- For the first objective, Section 2.1 presents a multi-class network equilibrium model to describe the flow distributions of both conventional vehicles (CVs) and AVs, given the presence of AV lanes in the network. Considering that the net benefit (e.g., reduced travel cost) derived from the deployment of AV lanes will further promote the AV adoption, Section 2.2 applies a diffusion model to forecast the evolution of AV market penetration. With the proposed equilibrium model and diffusion model, a time-dependent deployment model is then formulated in Section 2.3, which can be solved by an efficient solution algorithm.
- For the second objective, Section 3.1 illustrates the operational concept of AV zones and basic assumptions for the proposed models. Section 3.2 formulates the network equilibrium model and proposes its solution algorithm. Lastly, Section 3.3 optimizes the design of AV zones.

CHAPTER 1 BACKGROUND

Autonomous vehicles (AVs) are expected to offer extraordinary improvements to both the safety and efficiency of existing roadways and mobility systems. Although it will be many years before a widespread adoption of AV technology, recent developments suggest that they are fast-approaching. Google's AVs had driven more than 2,000,000 miles on public roads by June 2016 (Google Self-Driving Car Project, 2016). More recently, nuTonomy, a software company, has launched the world's first self-driving taxi in Singapore (nuTonomy, 2016). Many car manufactures, such as Volvo and Audi, are currently designing and testing their prototype AVs. In the United States, states such as Nevada, Florida, California, Michigan, and Washington D.C. have legalized AVs for testing on public roads. While thus far the development of AV technology appears to be primarily driven by the private sector, it is critical for government agencies to change various policies and practices to adapt to and further promote the deployment of the technology.

In this project, we advocate the need for infrastructure adaptation planning for AVs. Before manual driving can be completely phased out (or criminalized, as some have predicted), the traffic stream on a road network will still be heterogeneous, with both conventional vehicles (CVs) and AVs. We envision that government agencies can initially identify critical locations to implement various AV mobility applications. For example, a "bottleneck manager" can be implemented at a recurrent freeway bottleneck. When approaching, AVs send requests via vehicle-to-infrastructure wireless commutations to the "bottleneck manager," which will prioritize the requests and optimize their trajectories to ensure timely passage while preventing the bottleneck from being activated. To leverage the growing adoption of AVs, government agencies may later dedicate certain traffic lanes, highway segments or even areas of networks exclusively to AVs to facilitate the formulation of vehicle platoons to further improve throughput. Subsequently implemented are innovative control strategies that aim to achieve system optimum in those areas. The dedicated AV areas will expand gradually as the level of the market penetration of AVs increases and eventually support a fully connected and automated mobility in the whole system. Similar ideas have been suggested in the literature. For example, as current managed lanes are equipped with advanced communication and data transfer systems, researchers have suggested converting some of them into dedicated lanes for AVs to reduce congestion and improve the safety of passengers (Davis, 2014; Levin and Boyles, 2016a,b). To help boost the market penetration of AVs, Chen et al. (2016) proposed a time-dependent model to optimally deploy AV lanes on a general network consisting of both CVs and AVs. Godsmark and Kakkar (2014) pointed out that the presence of AV areas can maximize benefits brought by AVs as rapidly as possible, as well as promote the AV adoption.

This project first attempts to propose a general mathematical model to help government agencies optimally deploy AV lanes in a way to minimize the social cost. The decision-making process in such a planning practice possesses a structure of the leader-follower or Stackelberg game, in which government agencies serve as the leader and travelers are the follower. In order for government agencies to optimize those planning decisions, travelers' spontaneous responses need to be proactively considered in the optimization framework. This type of Stackelberg games have been formulated as mathematical programs with equilibrium constraints for many transportation applications (see, e.g., Wu et al., 2011, 2012; Yin et al., 2008; He et al., 2013a, 2015; Zhang et al., 2014; Chen et al., 2016). More specifically, given AV lanes deployed, we

assume that CVs and AVs follow the Wardrop equilibrium principle to choose their routes that minimize their individual travel costs (Wardrop, 1952), and the resulting flow distribution is in a multi-class network equilibrium (e.g., Yang and Meng, 2001; Wu et al., 2006). Furthermore, since the net benefit (e.g., reduced travel cost for AVs) derived from deploying AV lanes plays an important role in promoting the AV adoption, we apply a diffusion model to forecast the evolution of AV market penetration. Based on the network equilibrium model and diffusion model, we proposed a time-dependent deployment model to optimize the location design of AV lanes on a general transportation network. The AV market penetration follows a progressive process instead of a radical one, thus the AV lanes should also be deployed in a progressive fashion. More specifically, the optimized deployment plan will not only specify where and how many AV lanes to be deployed, but also when to deploy them.

In addition, this project deals with a particular issue in the infrastructure adaptation planning process and aims to present a mathematical framework for the optimal design of AV zones in a general network. With only AVs being allowed to enter, an AV zone consists of a set of links that are tailored to AVs. Note that in order not to compromise CVs' accessibility to various locations, the nodes within the zone in particular, the AV zone can be designed to consist of only urban expressways or arterial roads, excluding minor streets. It is assumed that within the zone, AVs cannot choose their routes. Instead, they report their exits and are then guided by a central controller to achieve the system optimum flow distribution in the zone. AV zones will enable full utilization of the AV technology within the zones to hopefully improve the performance of the whole network. These zones can help reduce travel times for AVs and further nurture the AV market. However, the existence of AV zones likely increases travel times for some CVs. Therefore, government agencies will need to make a tradeoff between these pros and cons in designing AV zones. The optimal design will depend on the market penetration of AVs, network topology and link characteristics, and more importantly, the route choices of both CVs and AVs in the network.

Similar to the deployment problem of AV lanes, optimal design of AV zones possesses a structure of leader-follower game, in which government agencies serve as the leader while CVs and AVs are the followers. Given a design of the AV zone, we firstly develop an innovative user equilibrium model we call the "mixed routing equilibrium model" to describe the flow distribution of AVs and CVs across the network. The novelty of the proposed model lies in the aspect that some paths consist of both links outside of and within the AV zones; AVs follow the user-optimum routing principle in the former and the system-optimum routing principle in the latter. This new equilibrium model is most relevant to mixed equilibrium models in the literature, e.g., Haurie and Marcotte (1985), Harker (1988), Yang and Zhang (2008), Zhang et al. (2008), and He et al. (2013b), where both the user-optimum and system-optimum route choice behaviors are considered. In all these previous models, all types of players share the same network, and each type of player applies a particular routing principle to traverse the whole network. In contrast, in our model, AVs and CVs may face different network topologies (recall that CVs are not allowed to enter AV zones) and, more importantly, AVs may apply different routing principles at different sub-networks. Mixed routing behaviors may become more relevant with the deployment of automated and connected vehicles. Capturing them in the network equilibrium framework is very challenging, which actually constitutes one of the major contributions of this project.

Given the proposed mixed routing equilibrium model, we proceed to optimize the deployment plan of AV zones over a general network. The design problem is formulated as a mixed-integer bi-level programing model that is very difficult to solve. The problem appears to have a similar structure as the cordon design problem for cordon congestion pricing (see, e.g., Zhang and Yang, 2004 and Sumalee, 2004), which was solved previously using genetic-algorithm-based heuristics, such as the cutset-based approach (Zhang and Yang, 2004), the branch-tree approach (Sumalee, 2004), and the Delaunay triangulation approach (Hult, 2006). However, most of the above algorithms have low efficiency on generating new feasible design plans. In this report, we adopt a simulated annealing algorithm or SAA (Kirkpatrick et al., 1983; Cerny, 1985) to solve the AV zone design problem, since a simple but efficient plan-updating strategy can be tailored for SAA in order to generate new feasible design plans efficiently.

For the remainder, Chapter 2 develops a mathematical approach to optimize a time-dependent deployment plan of AV lanes on a transportation network with heterogeneous traffic stream consisting of both conventional vehicles CVs and AVs, so as to minimize the social cost and promote the adoption of AVs. Chapter 3 presents a mathematical framework for the optimal design of AV zones in a general network. Concluding remarks are provided in Chapter 4.

CHAPTER 2 OPTIMAL DEPLOYMENT OF AUTONOMOUS VEHICLE LANES WITH ENDOGENOUS MARKET PENETRATION

In this chapter, Section 2.1 applies the multi-class network equilibrium model to describe the flow distributions of both CVs and AVs. Section 2.2 proposes the AV diffusion model to forecast the market penetration of AVs. Section 2.3 presents the mathematical program to optimize the AV-lane deployment plan, followed by numerical examples in Section 2.4.

Below are some notations used throughout the chapter.

Sets	
K	Set of paired links
N	Set of nodes
A	Set of links
$\hat{A}$	Set of AV links
M	Set of travel modes: mode 1 denotes CVs, and mode 2 denotes AVs
W	Set of origin-destination (OD) pairs
$P_\tau^{w,m}$	Set of paths for travel mode $m \in M$ between OD pair $w \in W$ at year $\tau \in T$
$\hat{P}_\tau^{w,m}$	Set of utilized paths for travel mode $m \in M$ between OD pair $w \in W$ at year $\tau \in T$
T	Set of years
Parameters	
m	Index of travel mode, $m \in M$
w	Index of OD pair, $w \in W$
p	Index of path, $p \in P_\tau^{w,m}$
d^{w*}	Potential AV market size for OD pair $w \in W$
γ_m	Value of time (VOT) for drivers of travel mode $m \in M$
σ	Interest rate
n	A factor converting social cost from an hourly basis to a yearly basis
τ	Index of year $\tau \in T$
ς	Unsafety factor for using CV
θ_a^k	If link a belongs to the kth link pair, and it is an AV link, then $\theta_a^k = 1$; If link a belongs to the kth link pair, and it is not an AV link, then $\theta_a^k = -1$; otherwise, $\theta_a^k = 0$
Variables	
$d_\tau^{w,m}$	Demand of travel mode $m \in M$ between OD pair $w \in W$ at year $\tau \in T$
$x_{a,\tau}^{w,m}$	Flow of travel mode $m \in M$ on link $a \in A$ between OD pair $w \in W$ at year $\tau \in T$
$v_{a,\tau}$	Aggregate flow on link $a \in A$ at year $\tau \in T$
y_τ^k	The number of lanes on the kth link pair that are converted into AV lanes at year $\tau \in T$
$C_\tau^{w,m}$	Equilibrium travel time for mode $m \in M$ between OD pair $w \in W$ at year $\tau \in T$

2.1 MULTI-CLASS NETWORK EQUILIBRIUM MODEL

Assume that the entire planning horizon is divided into $|T|$ years. Let $G(N, A)$ denote a general transportation network, where N and A are the sets of nodes and links in the network respectively. Let $\hat{A}$ represent the set of AV links in the network. Note that any link including AV lanes can be divided into one regular link and one AV link without affecting the network performance. For example, Figure 2-1(a) shows a simple network topology. If we consider link 1 and link 4 as the candidate links where AV lanes can be deployed, then its network topology can

be revised as the one in Figure 2-1(b). That is, $A = \{1,2,3,4,5,6,7\}$ and $\hat{A} = \{6,7\}$. We further define K as the set of these pairs of links. Specifically, in Figure 2-1(b), $K = \{(1,6),(4,7)\}$. We represent a link either as $a \in A$ or its starting and ending nodes, i.e., $a = (i,j) \in A$. Let $M = \{1,2\}$ denote the set of travel modes, in which mode 1 corresponds to CV and mode 2 corresponds to AV. The set of OD pairs is denoted as W, and $o(w)$ and $d(w)$ define the origin and destination of OD pair $w \in W$. The travel time of link $a \in A$ at year $\tau \in \Gamma$ is denoted as $t_{a,\tau}(v_{a,\tau})$, which is specified by the link performance function, e.g., in a form of the following function:

$$t_{a,\tau}(v_{a,\tau}) = t_a^0 \left[1 + \bar{\alpha}_a \left(\frac{v_{a,\tau}}{\Lambda_a^\tau}\right)^{\bar{\beta}_a}\right]$$

where t_a^0 is the free-flow travel time of link a; Λ_a^τ is the capacity of link a at year $\tau \in T$; $v_{a,\tau}$ is the link flow at year $\tau \in T$, and $\bar{\alpha}_a$ and $\bar{\beta}_a$ are two positive parameters.

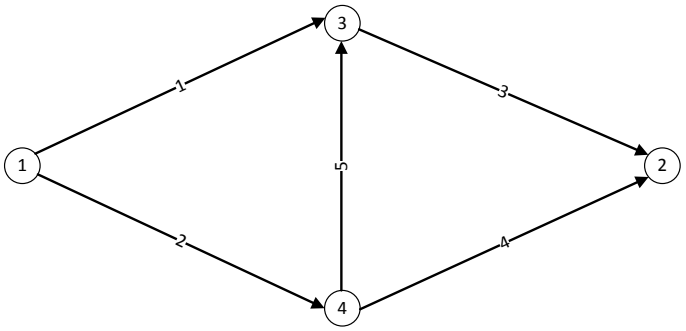

(a) Original network topology

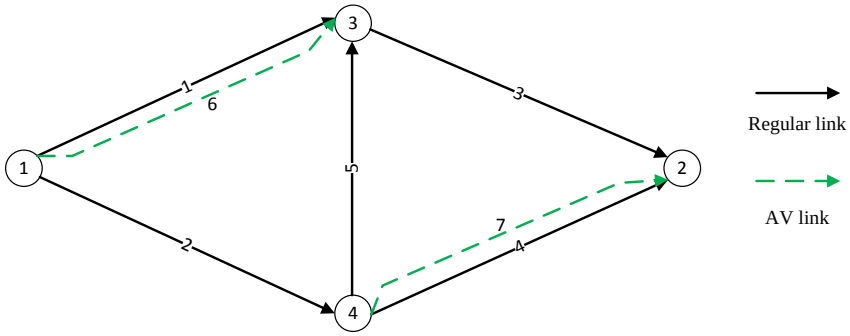

(b) Revised network topology

Figure 2-1. A simple network example

The flow distributions of both CVs and AVs at any year $\tau \in T$, can be described by the following network equilibrium model:

$$\boldsymbol{\Delta x}_\tau^{w,m} = \boldsymbol{E}^{w,m} d_\tau^{w,m} \qquad \forall w \in W, m \in M \qquad (2\text{-}1)$$

$$x_{a,\tau}^{w,2} \geq 0 \qquad \forall a \in A, w \in W \qquad (2\text{-}2)$$

$$x_{a,\tau}^{w,1} \geq 0 \qquad \forall a \in A \backslash \hat{A}, w \in W \qquad (2\text{-}3)$$

$$x_{a,\tau}^{w,1} = 0 \qquad \forall a \in \hat{A}, w \in W \qquad (2\text{-}4)$$

$$v_{a,\tau} = \sum_{m \in M} \sum_{w \in W} x_{a,\tau}^{w,m} \qquad \forall a \in A \qquad (2\text{-}5)$$

$$t_{a,\tau}(v_{a,\tau}) + \rho_{i,\tau}^{w,m} - \rho_{j,\tau}^{w,m} - \eta_{a,\tau}^{w,m} = 0 \qquad \forall a \in A, w \in W, m \in M \qquad (2\text{-}6)$$

$$\eta_{a,\tau}^{w,2} \cdot x_{a,\tau}^{w,2} = 0 \qquad \forall a \in A, w \in W \qquad (2\text{-}7)$$

$$\eta_{a,\tau}^{w,1} \cdot x_{a,\tau}^{w,1} = 0 \qquad \forall a \in A \backslash \hat{A}, w \in W \qquad (2\text{-}8)$$

$$\eta_{a,\tau}^{w,2} \geq 0 \qquad \forall a \in A, w \in W \qquad (2\text{-}9)$$

$$\eta_{a,\tau}^{w,1} \geq 0 \qquad \forall a \in A \backslash \hat{A}, w \in W \qquad (2\text{-}10)$$

where $\boldsymbol{\Delta}$ is the node-link incidence matrix associated with a given network, and $\boldsymbol{E}^{w,m}, w \in W, m \in M$ is a vector with a length of $|N|$. The vector consists of two non-zero components: one has a value of 1 corresponding to origin $o(w)$ and the other has a value of -1 corresponding to destination $s(w)$. $x_{a,\tau}^{w,m}$ is the link flow of mode $m \in M$ between O-D pair $w \in W$ at year $\tau \in T$, and $v_{a,\tau}$ is the aggregation of $x_{a,\tau}^{w,m}$ over all travel modes and OD pairs. Vectors $\boldsymbol{\rho}$ and $\boldsymbol{\eta}$ are auxiliary variables, and $\boldsymbol{\rho}$ represents the node potentials.

In the above, constraint (2-1) ensures the flow conservation; constraints (2-2) and (2-3) are nonnegative constraints on link flows; constraint (2-4) ensures that only AVs can use AV links; constraint (2-5) aggregates link flows across all travel modes and OD pairs; constraints (2-6)-(2-10) ensure that all utilized paths of the same travel mode between each OD pair share the same travel cost $\rho_{s(w),\tau}^{w,m} - \rho_{o(w),\tau}^{w,m}$, while those unutilized ones possess travel cost larger than or equal to $\rho_{s(w),\tau}^{w,m} - \rho_{o(w),\tau}^{w,m}$.

In addition, finding a solution to the system of equilibrium conditions is equivalent to solving the following mathematical problem (NE):

NE:

$$\min_{\mathbf{x}} \sum_{a \in A} \int_0^{v_{a,\tau}} t_{a,\tau}(x) dx$$

s.t. (2-1)-(2-5)

The equivalence can be established by comparing the KKT conditions of NE with the defined network equilibrium conditions (2-1)-(2-10).

2.2 AV DIFFUSION MODEL

Diffusion models have been widely applied to forecast how a new product or idea will be adopted over time. For example, Yang and Meng (2001) proposed a modified logistic growth model to investigate the adoption rate of advanced traveler information systems. Park et al.

(2011) proposed a diffusion model to simulate the market penetration of hydrogen fuel cell vehicles. Lavasani et al. (2016) developed a market penetration model to forecast the AV technology adoption by considering the price difference between AV and CV, as well as the economic wealth of the population. We here adopt the diffusion model proposed by Yang and Meng (2001). Specifically, the adoption of AVs at a given year depends on the adoption and the net benefit gained at the previous year. That is,

$$d_{\tau+1}^{w,2} = d_{\tau}^{w,2} + \mathrm{g}(\phi_{\tau}^{w}) d_{\tau}^{w,2}\left(1 - \frac{d_{\tau}^{w,2}}{d^{w*}}\right) \qquad \forall w \in W, \tau \in T\backslash\{|T|\} \qquad (2\text{-}11)$$

where d^{w*} is the potential AV market size for OD pair $w \in W$. Note that, the potential market size of a new product is predicted exogenously in many diffusion models (e.g., Lavasani et al., 2016; Park et al, 2011; Massiani and Gohs, 2015), with a few exception (Yang and Meng, 2001; Huang and Li, 2007). The latter ones relate the potential market penetration level to the benefit brought by the new product. Doing so, however, will complicate the AV-lane deployment model (proposed in Section 4), and even make it intractable. Therefore, in this chapter, we adopt a fixed potential AV market size for each OD pair. $\mathrm{g}(\phi_{\tau}^{w})$ is the intrinsic variable growth coefficient for OD pair $w \in W$, which is defined as follows:

$$\mathrm{g}(\phi_{\tau}^{w}) = \hat{a} e^{\hat{b}(\phi_{\tau}^{w} - \bar{\phi}^{w})} \qquad \forall w \in W, \tau \in T \qquad (2\text{-}12)$$

where $\hat{a}$ and $\hat{b}$ are two parameters ($\hat{a} > 0$; $\hat{b} \geq 0$), $\bar{\phi}^{w}$ is the OD specific benefit threshold for OD pair $w \in W$, and ϕ_{τ}^{w} is the net benefit gained for OD pair $w \in W$ at year $\tau \in T$. ϕ_{τ}^{w} is defined as follows:

$$\phi_{\tau}^{w} = \left[(\gamma_1 + \varsigma) C_{\tau}^{w,1} - \gamma_2 C_{\tau}^{w,2}\right] \cdot L_{\tau}^{w} - Y_{\tau} \qquad \forall w \in W, \tau \in T \qquad (2\text{-}13)$$

where γ_m is the value of travel time for travel mode m, ς is a nonnegative unsafety factor for using CVs compared with using AVs, L_{τ}^{w} is the number of trips between OD pair $w \in W$ at year $\tau \in T$, which could be the average annual trip number obtained from household travel survey, Y_{τ} is the additional annual cost for using AVs at year $\tau \in T$, and $C_{\tau}^{w,m}$ is the equilibrium travel time of mode $m \in M$ between OD pair $w \in W$ at year $\tau \in T$, i.e.,

$$C_{\tau}^{w,m} = \rho_{s(w),\tau}^{w,m} - \rho_{o(w),\tau}^{w,m} \qquad \forall m \in M, w \in W, \tau \in T \qquad (2\text{-}14)$$

where $\boldsymbol{\rho}$ can be obtained by solving NE.

Without loss of generality, we assume that the yearly travel demand between each OD pair remains the same during the entire planning horizon. That is,

$$\sum_{m \in M} d_{\tau}^{w,m} = \sum_{m \in M} d_{0}^{w,m} \qquad \forall w \in W, \tau \in T \qquad (2\text{-}15)$$

2.3 AV-LANE LOCATION PROBLEM

In this section, we will investigate how to optimally locate AV lanes to minimize the social cost with the consideration of the market penetration of AVs. AV lanes can only be located to a given set of candidate links, to reflect possible restrictions imposed in field applications. The optimal deployment problem of AV lanes will be formulated as a bi-level model. The lower-level problem is the multi-class network equilibrium defined in Eqs. (2-1)-(2-10), while the upper-level one investigates when, where and how many AV lanes should be deployed.

2.3.1 Model Formulation

Let θ_a^k denote the pair-link incidence. If link a belongs to the kth pair of links, and it is an AV link, then $\theta_a^k = 1$; if it is a regular link, then $\theta_a^k = -1$; otherwise, $\theta_a^k = 0$. Further, let y_τ^k be an integer variable, representing the number of lanes on the kth pair of links that are converted from regular lanes to AV lanes at year τ. Then, the AV-lane location problem (AVLL) can be formulated as follows:

AVLL:

$$\min_{\boldsymbol{x},\boldsymbol{d},\boldsymbol{\eta},\boldsymbol{\rho},\boldsymbol{y}} \sum_{\tau\in T}\sum_{w\in W}\left[\sum_{m\in M} n\frac{\left((\gamma_1+\varsigma)d_\tau^{w,1}C_\tau^{w,1}+\gamma_2 d_\tau^{w,2}C_\tau^{w,2}\right)}{(1+\sigma)^{\tau-1}}\right]$$

s.t. (2-1)-(2-15)

$$\Lambda_a^\tau = \bar{\Lambda}_a + \bar{c}_a \cdot \sum_{k\in K}\theta_{a,k}\sum_{j=1}^{\tau} y_j^k \qquad \forall a\in A, \tau\in T \qquad (2\text{-}16)$$

$$\bar{\Lambda}_a + \bar{c}_a \cdot \sum_{k\in K}\theta_{a,k}\sum_{j=1}^{|T|} y_j^k \geq \mu_a \qquad \forall a\in A \qquad (2\text{-}17)$$

$$y_\tau^k \in \{0,1,\dots,I_k\} \qquad \forall k\in K, \tau\in T \qquad (2\text{-}18)$$

where σ is the discount rate per year, n is a factor converting social cost from an hourly basis to a yearly basis, μ_a is a given parameter, representing the minimum capacity required for link a, I_k is a given integer, representing the maximum number of AV lanes that can be deployed on the kth pair of links each year, $\bar{\Lambda}_a$ is the initial capacity of link a, $\bar{c}_a$ is the per-lane capacity of link a, thus $\bar{\Lambda}_a + \bar{c}_a \cdot \sum_{k\in K}\theta_{a,k}\sum_{j=1}^{\tau} y_{k,j}$ represents the capacity of link a at year τ. It should be noted that the increase of AV-link capacity and the decrease of the paired regular-link capacity is not symmetric, as their per-lane capacities are not the same. As mentioned before, the per-lane capacity can become tripled when it is converted from a regular lane to an AV lane due to the benefits from vehicle-to-vehicle communication.

In the above, the objective function is to minimize the total social cost, consisting of the costs of both CVs and AVs; constraint (2-16) calculates the capacity of link a at year τ; constraint (2-17) ensures that the capacity of link a should be no less than a required minimum

capacity. For example, in order to maintain the accessibility of the network, there must be at least one regular lane for all the regular links, otherwise, CVs of some OD pairs cannot finish their trips. Constraint (2-18) implies that y_τ^k must be an integer number, and its upper bound is I_k.

The above model can be readily extended to consider the construction cost for the AV-lane deployment and the government subsidy, via adding a term $\sum_\tau \frac{\Pi_\tau}{(1+\sigma)^{\tau-1}} - \sum_\tau \frac{S_\tau}{(1+\sigma)^{\tau-1}}$ to the objective function, where Π_τ and S_τ are the construction cost and the government subsidy at year τ respectively.

2.3.2 Solution Algorithm

The AVLL problem can be generally categorized as a discrete network design problem (DNDP). And those solution algorithms proposed in the literature for DNDP can be employed to solve AVLL, e.g., branch-and-bound technique (LeBlanc, 1975), support-function based method (Gao et al., 2005), active-set algorithm (Zhang et al., 2009), system optimal-relaxation based method and user equilibrium-reduction based method (Wang et al., 2013). Here, AVLL is in form of a mathematical program with complementarity constraints (see, e.g., Luo et al., 1996), we employ the active-set algorithm developed by Zhang et al. (2009) to solve it. The basic idea is to solve a sequence of restricted nonlinear problems to obtain a strongly stationary solution to the original AVLL.

Let Φ_k denote the smallest integer number such that $I_k \le 2^{\Phi_k} - 1$, then constraint (2-18) can be represented as $y_\tau^k = \sum_{\varpi=1}^{\Phi_k} y_\tau^{k,\varpi}\, 2^{\varpi-1}$, where $y_\tau^{k,\varpi}$ is a binary variable for $\varpi \in \{1, \dots, \Phi_k\}$.

For a particular deployment plan, we define $|T|$ pairs of active sets, $\Omega_{\tau,0} = \{(k,\varpi): y_\tau^{k,\varpi} = 0\}$ and $\Omega_{\tau,1} = \{(k,\varpi): y_\tau^{k,\varpi} = 1\}, \forall \tau \in T$. These two sets should be "complete", i.e., $\Omega_{\tau,0} \cup \Omega_{\tau,1} = \{(k,\varpi)\};\ \Omega_{\tau,0} \cap \Omega_{\tau,1} = \emptyset, \forall \tau \in T$. Given some deployment plan $\cup_{\tau\in\Gamma} (\Omega_{\tau,0}, \Omega_{\tau,1})$, the restricted AVLL (RAVLL) problem can be formulated as below:

RAVLL:

$$\min_{\boldsymbol{x},\boldsymbol{d},\boldsymbol{\eta},\boldsymbol{\rho},\boldsymbol{y}} \sum_{\tau\in T}\sum_{w\in W}\left[\sum_{m\in M} n \frac{\left((\gamma_1+\varsigma) d_\tau^{w,1} C_\tau^{w,1} + \gamma_2 d_\tau^{w,2} C_\tau^{w,2}\right)}{(1+\sigma)^{\tau-1}}\right]$$

s.t. (2-1)-(2-15)

$$\Lambda_a^\tau = \bar{\Lambda}_a + \bar{c}_a \cdot \sum_{k\in K} \theta_{a,k} \sum_{j=1}^{\tau}\sum_{\varpi}^{\Phi_k} y_j^{k,\varpi} \qquad \forall a \in A, \tau \in T \qquad (2\text{-}19)$$

$$\bar{\Lambda}_a + \bar{c}_a \cdot \sum_{k\in K} \theta_{a,k} \sum_{j=1}^{|T|}\sum_{\varpi}^{\Phi_k} y_j^{k,\varpi} \ge \mu_a \qquad \forall a \in A \qquad (2\text{-}20)$$

$$y_\tau^{k,\varpi} = 0 \qquad \forall (k,\varpi) \in \Omega_{\tau,0}, \tau \in T \qquad (2\text{-}21)$$

$$y_\tau^{k,\varpi} = 1 \qquad \forall (k,\varpi) \in \Omega_{\tau,1}, \tau \in T \qquad (2\text{-}22)$$

Although RAVLL is another mathematical problem with complementarity constraints, its optimal solution can be easily obtained by solving the NE problem, with the deployment plan fixed. Below is the procedure of the active-set algorithm. The convergence of the algorithm has been proved by Zhang et al. (2009), thus is not presented here.

Step 0: Set $\epsilon = 1$ and solve NE with an initial deployment plan $\cup_{\tau \in T} \left(\Omega_{\tau,0}^1, \Omega_{\tau,1}^1\right)$ for each year $\tau \in T$.

Step 1: Construct a solution $(\boldsymbol{x}, \boldsymbol{d}, \boldsymbol{\eta}, \boldsymbol{\rho}, \boldsymbol{y})^T$ to RAVLL based on the optimal solutions derived from solving NE with $\cup_{\tau \in T} \left(\Omega_{\tau,0}^\epsilon, \Omega_{\tau,1}^\epsilon\right)$. Then, solve RAVLL to determine $\lambda_{k,\varpi,\tau}^\epsilon$ and $\mu_{k,\varpi,\tau}^\epsilon$, the Lagrangian multipliers associated with constraints (2-21) and (2-22). Set $TT^\epsilon = \sum_{\tau \in T} \sum_{w \in W} \left[\sum_{m \in M} n \frac{\left((\gamma_1 + \varsigma) d_\tau^{w,1} C_\tau^{w,1} + \gamma_2 d_\tau^{w,2} C_\tau^{w,2}\right)}{(1+\sigma)^{\tau-1}} \right]$.

Step 2: Set $Q = -\infty$ and adjust the active sets by performing the following steps:

a) Let $\left(\hat{\boldsymbol{z}}, \hat{\boldsymbol{h}}\right)$ solve the following knapsack problem:

$$\min \sum_{\tau \in T} \sum_{(k,\varpi) \in \Omega_{\tau,0}^\epsilon} \lambda_{k,\varpi,\tau}^\epsilon z_{k,\varpi,\tau} - \sum_{\tau \in T} \sum_{(k,\varpi) \in \Omega_{\tau,1}^\epsilon} \mu_{k,\varpi,\tau}^\epsilon h_{k,\varpi,\tau}$$

s.t.

$$\bar{\Lambda}_a + \bar{c}_a \cdot \sum_{\tau \in T} \left[\sum_{(k,\varpi) \in \Omega_{\tau,1}^\epsilon} \theta_{a,k} 2^{\varpi-1} + \sum_{(k,\varpi) \in \Omega_{\tau,0}^\epsilon} \theta_{a,k} z_{k,\varpi,\tau} 2^{\varpi-1} - \sum_{(k,\varpi) \in \Omega_{\tau,1}^\epsilon} \theta_{a,k} h_{k,\varpi,\tau} 2^{\varpi-1} \right] \geq \mu_a, \forall a \in A$$

$$\sum_{\tau \in T} \sum_{(k,\varpi) \in \Omega_{\tau,0}^\epsilon} \lambda_{k,\varpi,\tau}^\epsilon z_{k,\varpi,\tau} - \sum_{\tau \in T} \sum_{(k,\varpi) \in \Omega_{\tau,1}^\epsilon} \mu_{k,\varpi,\tau}^\epsilon h_{k,\varpi,\tau} \geq Q$$

$$z_{k,\varpi,\tau}, h_{k,\varpi,\tau} \in \{0,1\}$$

If its optimal objective value is zero, stop and the current solution is optimal. Otherwise, go to Step 2b.

b) Set:

i. $D = \sum_{\tau \in T} \sum_{(k,\varpi) \in \Omega_{\tau,0}^\epsilon} \lambda_{k,\varpi,\tau}^\epsilon \hat{z}_{k,\varpi,\tau} - \sum_{\tau \in \Gamma} \sum_{(k,\varpi) \in \Omega_{\tau,1}^\epsilon} \mu_{k,\varpi,\tau}^\epsilon \hat{h}_{k,\varpi,\tau}$,

ii. $\widehat{\Omega}_{\tau,0} = \left(\Omega_{\tau,0}^\epsilon - \left\{(k,\varpi) \in \Omega_{\tau,0}^\epsilon : \hat{z}_{k,\varpi,\tau} = 1\right\}\right) \cup \left\{(k,\varpi) \in \Omega_{\tau,1}^\epsilon : \hat{h}_{k,\varpi,\tau} = 1\right\}, \forall \tau \in T$,

iii. $\widehat{\Omega}_{\tau,1} = \left(\Omega_{\tau,1}^{\epsilon} - \left\{(k,\varpi) \in \Omega_{\tau,1}^{\epsilon} : \hat{h}_{k,\varpi,\tau} = 1\right\}\right) \cup \left\{(k,\varpi) \in \Omega_{\tau,0}^{\epsilon} : \hat{z}_{k,\varpi,\tau} = 1\right\}, \forall \tau \in T.$

c) Solve NE with a deployment plan $\hat{\mathbf{y}}$ compatible with $\cup_{\tau \in T} \left(\widehat{\Omega}_{\tau,0}, \widehat{\Omega}_{\tau,1}\right)$. If its social cost $TT < TT^{\epsilon}$, go to Step 2d since the location plan $\cup_{\tau \in T} \left(\widehat{\Omega}_{\tau,0}, \widehat{\Omega}_{\tau,1}\right)$ leads to a decrease in the social cost. Otherwise, set $Q = D + \varepsilon$, where $\varepsilon > 0$ is sufficiently small, and return to Step 2a.

d) Set $\Omega_{\tau,0}^{\epsilon+1} = \widehat{\Omega}_{\tau,0}$, $\Omega_{\tau,1}^{\epsilon+1} = \widehat{\Omega}_{\tau,1}$, $\forall \tau \in T$, and $\epsilon = \epsilon + 1$. Go to Step 1.

2.4 NUMERICAL EXAMPLES

2.4.1 Basic Settings

The numerical examples are conducted based on the south Florida network as shown in Figure 2-2, which consists of 232 regular links, 44 AV links, 82 nodes and 83 OD pairs. The OD demand is given in Table 2-1 and link characteristics are omitted due to space limitation. Table 2-2 shows the paired links, in which each AV link is paired with one regular link. For example, link 233 is an AV link, and link 15 is the paired regular link. They have the same link characteristics except the initial number of lanes and per-lane capacity. Specifically, the initial capacities of AV links are set as 0, meaning that without deploying AV lanes, the AV links are only virtual links, which can not be utilized.

We assume that the initial adoption rate of AVs for each OD pair is 2%, and the potential market size is 75% (Lavasani et al., 2016). The default model parameters include: (1) discount rate: $\sigma = 0.03$; (2) converting factor: $n = 365 \times 24 = 8{,}760$ (hour/year); (3) per-lane capacity of a regular link: $\bar{c}_a, \forall a \in A \backslash \hat{A}$, equal to the link capacity divided by the number of lanes on that link; (4) per-lane capacity of an AV link: $\bar{c}_a, \forall a \in \hat{A}$, equal to 2.5 times the per-lane capacity of the paired regular link; (5) planning horizon: $|T| = 40$; (6) the number of trips: $L_{\tau}^{w} = 720$ (trips/year), $\forall w \in W, \tau \in \Gamma$; (7) additional annual cost for using AVs: $Y_{\tau} = 1{,}000$ ($/year), $\forall \tau \in \Gamma$; (8) OD specific benefit threshold: $\bar{\phi}^{w} = 1{,}000$ ($), $\forall w \in W$; (9) VOT: $\gamma_1 = 0.5$ and $\gamma_2 = 0.5$ ($/min); (10) unsafety factor for using CV: $\varsigma = 0.1$ ($/min); (11) two parameters in Eq. (11): $\hat{a} = 0.3$(1/year), $\hat{b} = 0.00005$(year/$); (12) minimum link capacity: $\mu_a = \bar{c}_a, \forall a \in A \backslash \hat{A}$, and $\mu_a = 0, \forall a \in \hat{A}$; (13) maximum number of AV lanes can be deployed each year: $I_k = 3, \forall k \in K$. It should be noted that all the above values are chosen for illustrative purpose.

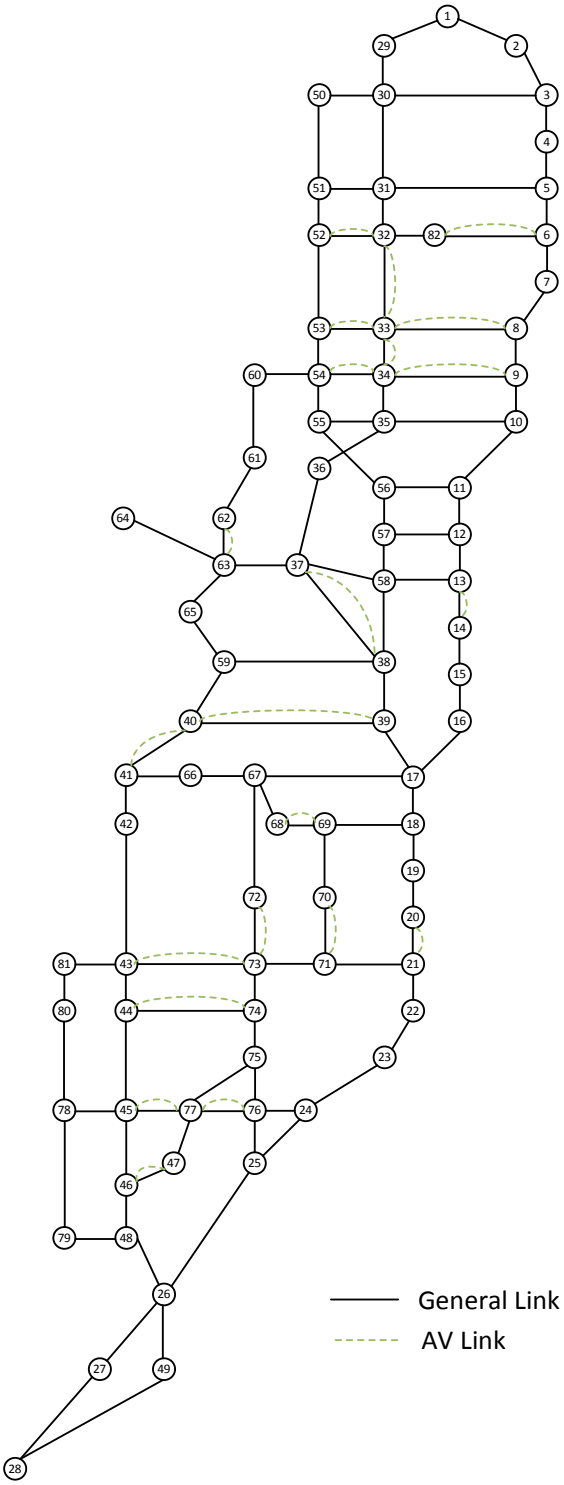

Figure 2-2. South Florida network

Table 2-1. OD demand of south Florida network

OD	Demand	OD	Demand	OD	Demand	OD	Demand
1-36	743.56	28-57	743.56	50-19	793.76	64-30	815.30
1-57	860.80	28-63	863.41	50-59	758.15	66-31	768.05
4-64	810.61	29-37	794.11	50-69	806.96	68-5	801.23
5-40	837.18	29-62	806.96	51-21	804.53	70-82	802.10
5-41	862.89	31-70	770.49	51-23	760.76	74-8	826.94
6-42	823.64	32-24	763.02	52-44	768.92	74-33	843.44
7-72	809.91	32-76	848.65	52-71	757.29	75-33	832.32
8-47	847.60	32-80	824.16	53-24	820.68	76-8	777.95
9-46	847.08	33-74	752.60	53-46	798.97	76-33	842.74
10-45	825.72	34-48	812.35	53-75	766.84	76-53	816.17
12-28	810.09	36-1	845.87	54-45	835.45	78-35	828.85
13-2	823.98	40-30	789.77	54-78	841.53	78-53	769.79
14-1	854.38	41-51	846.91	55-48	765.62	78-55	759.89
19-4	843.26	43-7	802.79	55-79	862.37	81-8	767.19
19-50	856.46	44-82	864.97	57-1	832.84	81-33	845.00
21-51	861.33	45-54	803.49	58-29	774.83	81-52	826.07
24-53	786.64	46-53	745.82	60-1	836.84	82-22	763.89
24-82	797.93	48-8	812.00	61-1	746.69	82-42	838.40
26-9	825.72	48-55	768.75	61-27	782.30	82-74	811.30
26-10	781.78	49-10	749.82	61-49	815.12	82-80	766.67
28-56	839.27	49-34	865.49	63-29	776.22		

Table 2-2. AV links and their paired links

Pair	AV link	Paired link	Pair	AV link	Paired link	Pair	AV link	Paired link
1	233	15	16	248	94	31	263	178
2	234	20	17	249	102	32	264	180
3	235	23	18	250	105	33	265	194
4	236	34	19	251	111	34	266	196
5	237	36	20	252	112	35	267	199
6	238	52	21	253	113	36	268	201
7	239	53	22	254	116	37	269	204
8	240	84	23	255	123	38	270	205
9	241	85	24	256	127	39	271	207
10	242	87	25	257	130	40	272	209
11	243	88	26	258	133	41	273	217
12	244	89	27	259	135	42	274	218
13	245	90	28	260	147	43	275	221
14	246	91	29	261	150	44	276	231
15	247	92	30	262	153			

2.4.2 Plan Comparison

In this section, we consider three different deployment plans to demonstrate how an appropriate plan can benefit the system performance. The first plan is to do nothing, meaning that no AV lanes will be deployed; the second plan is listed in Table 2-3; and the third plan is to deploy all the AV lanes in Table 2-3 at the first year (see Table 2-4). The social costs associated with these three plans are calculated to be $\$6.845 \times 10^{11}$, $\$6.582 \times 10^{11}$, and $\$6.814 \times 10^{11}$, respectively. As can be observed, although the number of AV lanes and their locations are exactly the same for plan 2 and plan 3, the performance of plan 2 is much better than that of plan 3 in term of the social cost. Compared with plan 1 (to do nothing), the former reduces the social cost by 3.84%, while the latter only leads to a reduction of 0.45%. It implies that considering the time dimension into the deployment plan is of critical importance.

Table 2-3. Deployment plan 2

Pair	τ	Number of AV lanes deployed	Pair	τ	Number of AV lanes deployed	Pair	τ	Number of AV lanes deployed
2	21	1	13	10	1	22	11	1
3	10	1	13	11	1	22	12	1
4	11	1	14	12	1	23	25	2
4	12	3	15	9	1	26	22	1
5	11	3	15	11	1	27	35	1
5	12	1	16	13	1	29	13	2
5	17	1	17	10	1	30	13	1
8	10	1	17	11	1	37	35	3
8	11	1	18	10	1	37	36	1
10	35	1	18	11	1	37	37	1
10	36	1	19	10	1	39	35	3
11	10	1	20	15	1	39	36	2
11	11	1	21	12	1	42	1	2
12	11	2	21	13	1			

Table 2-4. Deployment plan 3

Pair	τ	Number of AV lanes deployed	Pair	τ	Number of AV lanes deployed	Pair	τ	Number of AV lanes deployed
2	1	1	14	1	1	23	1	2
3	1	1	15	1	2	26	1	1
4	1	4	16	1	1	27	1	1
5	1	5	17	1	2	29	1	2
8	1	2	18	1	2	30	1	1
10	1	2	19	1	1	37	1	5
11	1	2	20	1	1	39	1	5
12	1	2	21	1	2	42	1	2
13	1	2	22	1	2			

We further examine the evolution of AV market penetration and the annual cost under the three plans, as displayed in Figure 2-3 and Figure 2-4. It can be observed that the adoption rate resulted from plan 3 grows the fastest, which is easy to understand since plan 3 provides all the capacity for AVs at the very beginning of the modeling horizon. The annual costs for the first four years under plan 3 are much higher than those under the other two plans. The reason behind is when the level of market penetration of AVs is low, although deploying all the AV lanes can help to enlarge the gain of this portion of vehicles, it will lead to tremendous increase in the travel time of CVs. As a result, the total social welfare decreases. What's worse, as shown in Figure 2-4, such negative effect can last for several years as it takes time for CV drivers to adopt AVs. On the contrary, although plan 2 does not promote the adoption rate as quickly as plan 3, it does reduce the social cost by a larger amount via deploying AV lanes progressively. It is worthwhile to highlight that, in plan 2, most of the AV lanes are deployed after the 10^{th} year when the AV market penetration is high enough, i.e., 26% (see Figure 2-3). When the market penetration of AVs is low (e.g., at the first several years), only two AV lanes are deployed (see Table 2-3).

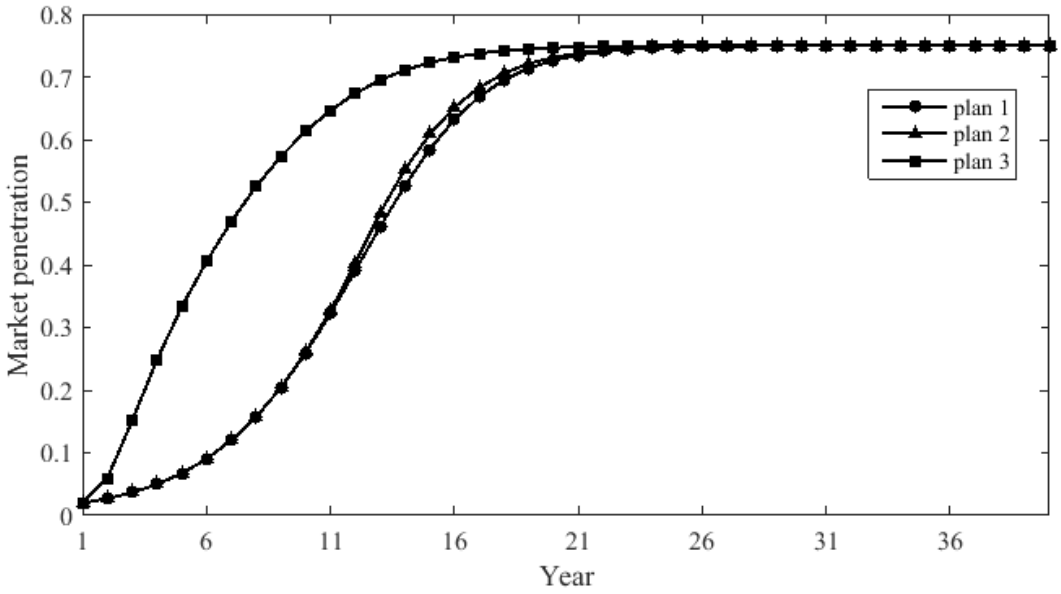

Figure 2-3. Evolution of AV market penetration under various plans

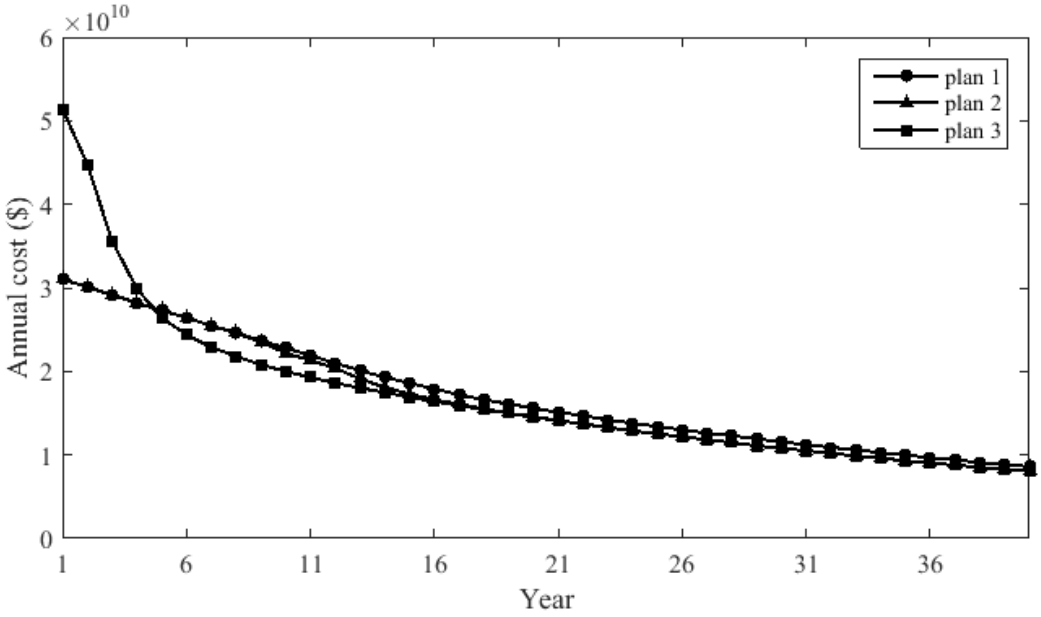

Figure 2-4. Evolution of annual cost under various plans

2.4.3 Sensitivity Analysis

As many parameters have impact on the market penetration of AVs, sensitivity analysis is conducted in this section. All the numerical experiments in this section are based on plan 2.

Figure 2-5 shows the AV market penetration curves with variable capacity ratios between AV lanes and regular lanes. Specifically, "3.0 times" means that the per-lane capacity becomes tripled when it is converted from a regular lane to an AV lane. Interestingly, although the growth rate increases as the capacity ratio increases, the differences among them are indistinctive in Figure 2-5, which indicates that increasing the per-lane capacity of AV lanes will not significantly promote the market penetration. It makes sense because the coverage area of AV links is relatively small, thus increasing their capacities only leads to limited reduction in the AVs' trip times. Actually, the total social costs associated with "1.5 times", "2.0 times", "2.5 times", and "3.0 times" are $\$6.693 \times 10^{11}$, $\$6.619 \times 10^{11}$, $\$6.582 \times 10^{11}$, and $\$6.562 \times 10^{11}$, respectively. The variance is very small.

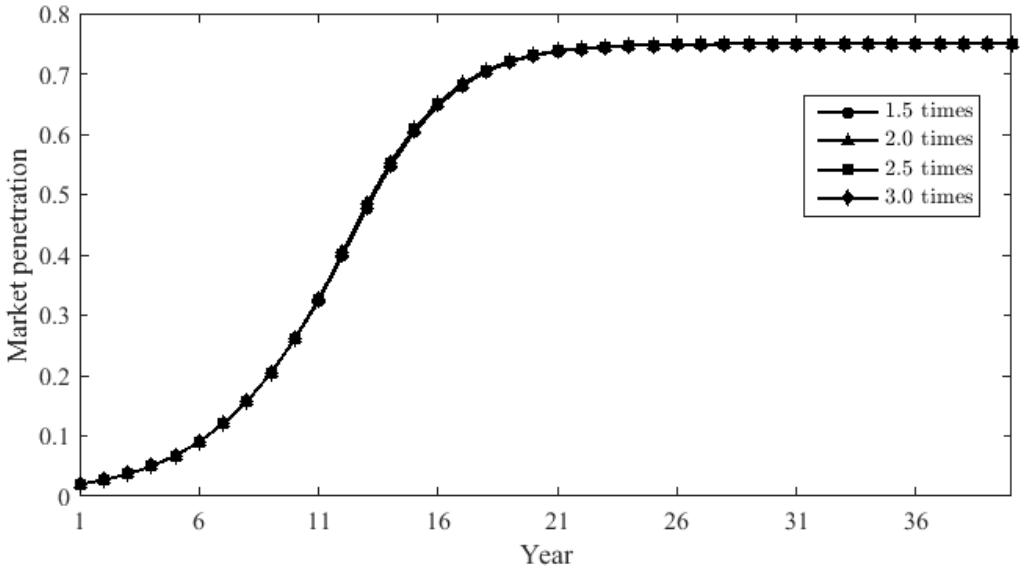

Figure 2-5. Evolution of AV market penetration with variable ratios of AV-lane capacity over regular-lane capacity

Figure 2-6 specifies the evolution of AV market penetration with different unsafety factors (i.e., ς). As ς increases, the growth rate increases, and it takes fewer years to reach the potential market size. The reason is straightforward: when the unsafety factor of using CVs becomes larger, the incentive for people to adopt AVs will be higher.

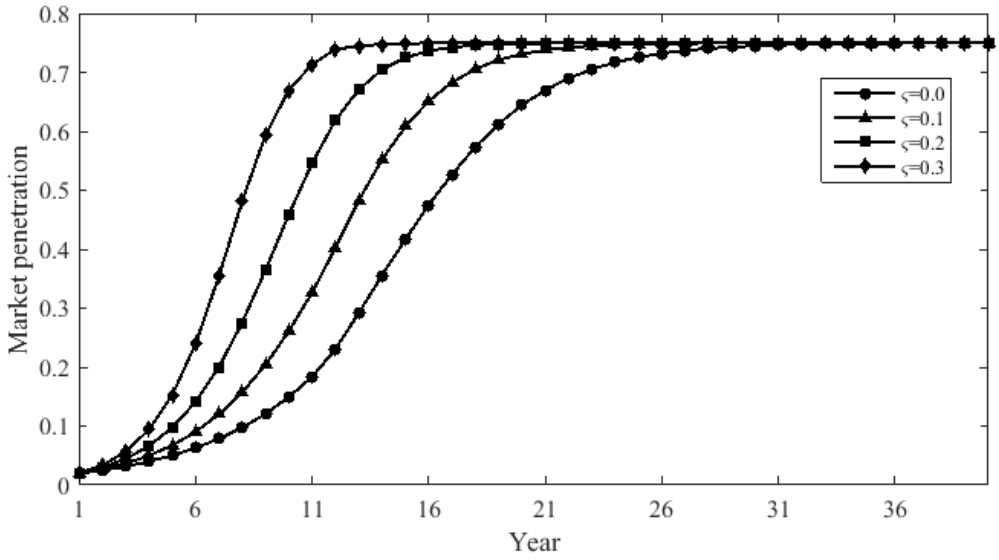

Figure 2-6. Evolution of AV market penetration with different unsafety factors

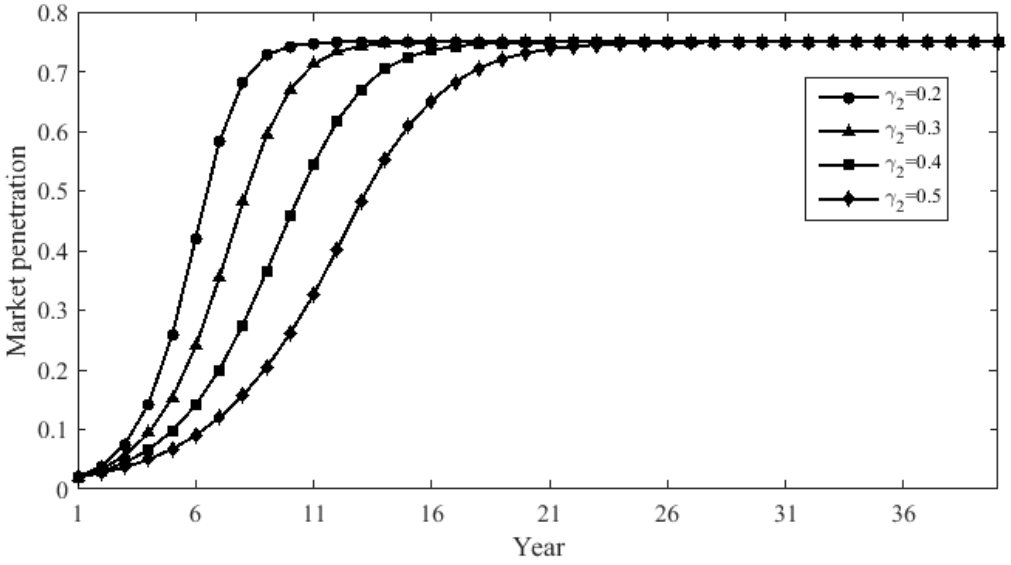

Figure 2-7. Evolution of AV market penetration with different VOTs of AVs

Traveling with AVs, people can concentrate on dealing with other personal matters instead of driving, thus their VOTs (i.e., γ_2) are envisioned to be no greater than those traveling with CVs (i.e., γ_1). To examine how γ_2 affects the AV adoption rate, Figure 2-7 plots the penetration curves with various γ_2. It can be observed that as γ_2 increases, the growth rate increases, and the time to reach the saturation point becomes shorter. For example, when $\gamma_2 = 0.2$ (\$/min), it only takes 12 years to reach the saturation point, which is only half of the time

needed when $\gamma_2 = 0.5$ ($/min). Accordingly, we may expect that the higher autonomous level of AVs is, the higher adoption rate will be.

To enable full-autonomous driving, intelligent control systems and various types of sensors (e.g., cameras, radar, and ultrasonic sensors) are required. Consequently, AVs are usually more expensive to use than CVs, and the additional costs become a critical factor preventing people from adopting AVs. Figure 2-8 describes how the evolution curve of AV market penetration changes with changing additional annual cost. As expected, higher additional annual costs will lead to lower growth rates. However, the saturation points do not vary much with different additional annual costs. Specifically, it takes about 26 years to achieve the potential market size for all scenarios.

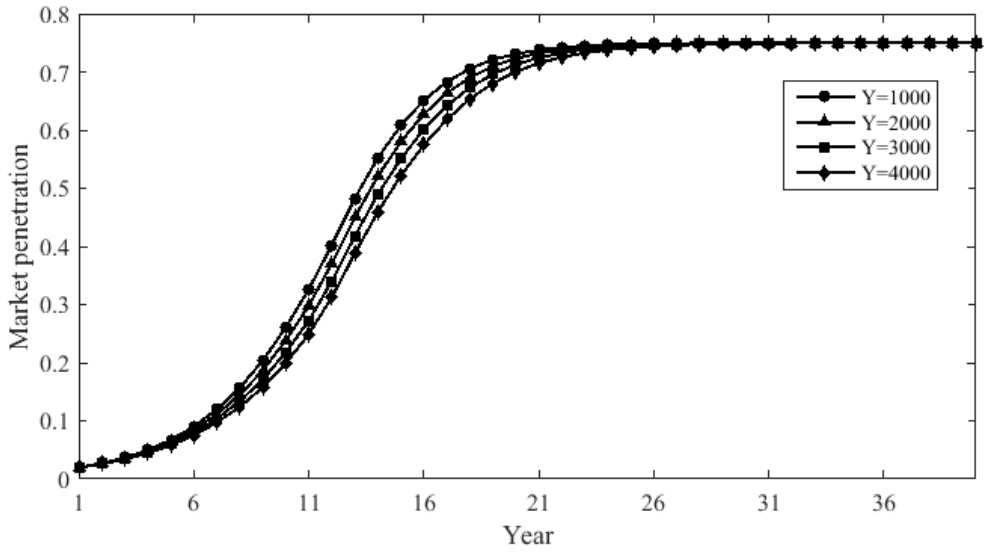

Figure 2-8. Evolution of AV market penetration with different additional annual costs for using AVs

As the number of annual trips varies from person to person, Figure 2-9 illustrates its impact on the AV market evolution. As can be seen, increasing the number of annual trips results in increased adoption rate of AVs, as well as fewer years to reach the saturation point. This is because more benefit can be derived when more trips are involved as per Eq. (13).

To investigate the impact of the potential market size on the market penetration curve, simulation experiments based on four potential market sizes: 65%, 75%, 85%, and 95% are conducted. Figure 2-10 illustrates the associated evolution patterns of AV market penetration. All patterns have similar growth rates in the earlier years (e.g., year 1 to10), while the growth rates diverge in the later years, and higher potential market sizes lead to larger growth rates. It is worthwhile to point out that the saturation points associated with different potential market sizes do not vary much, which is in agreement with the finding of Lavasani et al. (2016)

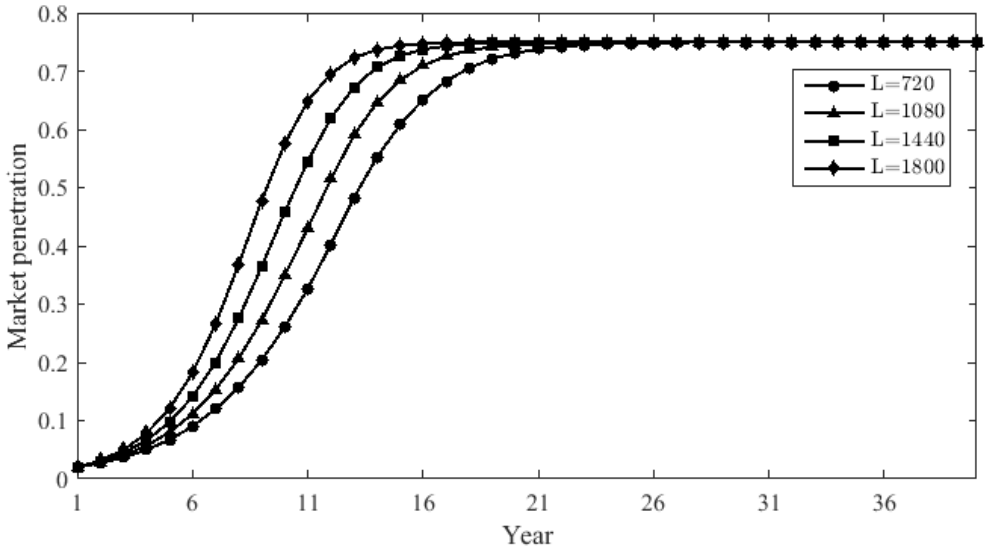

Figure 2-9. Evolution of AV market penetration with different numbers of annual trips

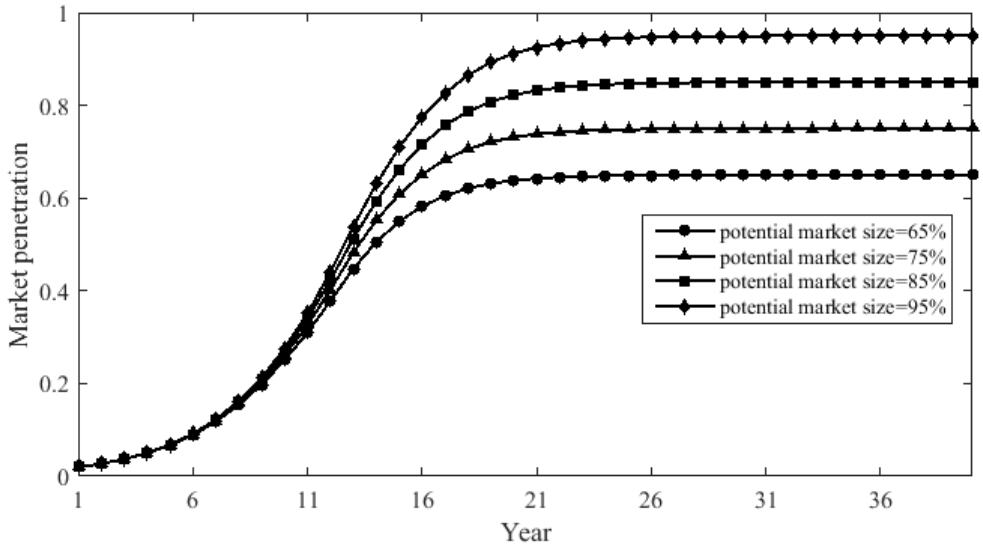

Figure 2-10. Evolution of AV market penetration with different potential market sizes

2.4.4 Optimal Location Plan

In this section, we solve AVLL for the south Florida network. Instead of starting with only one initial deployment plan, we start with different initial plans for the active-set algorithm, and take the best optimal plan as the final solution. By doing so, some poor local solution can be avoided. The final deployment plan obtained is given in Table 2-5, and the associated social cost is $\$6.578 \times 10^{11}$. Compared with plan 1 (to do nothing), the optimal plan reduces the social cost by $\$2.674 \times 10^{10}$ or 3.91%. Figure 2-11 and Figure 2-12 illustrate the evolution of AV market

penetration and annual cost under both the optimal plan and plan 1. As we can see, the optimal plan does not lead to reduced annual cost until the 9th year, when the AV market penetration reaches a relative high rate.

Table 2-5. Optimal deployment plan

Pair	τ	Number of AV lanes deployed	Pair	τ	Number of AV lanes deployed	Pair	τ	Number of AV lanes deployed
2	21	2	13	10	2	21	12	2
3	1	1	14	12	1	22	9	1
4	12	3	15	8	1	22	11	1
4	26	1	15	11	1	23	25	2
5	11	3	16	13	1	26	22	1
5	13	2	17	10	2	29	13	2
8	9	2	18	10	2	30	13	1
11	10	2	19	10	1	42	1	1
12	11	2	20	15	1	42	2	1

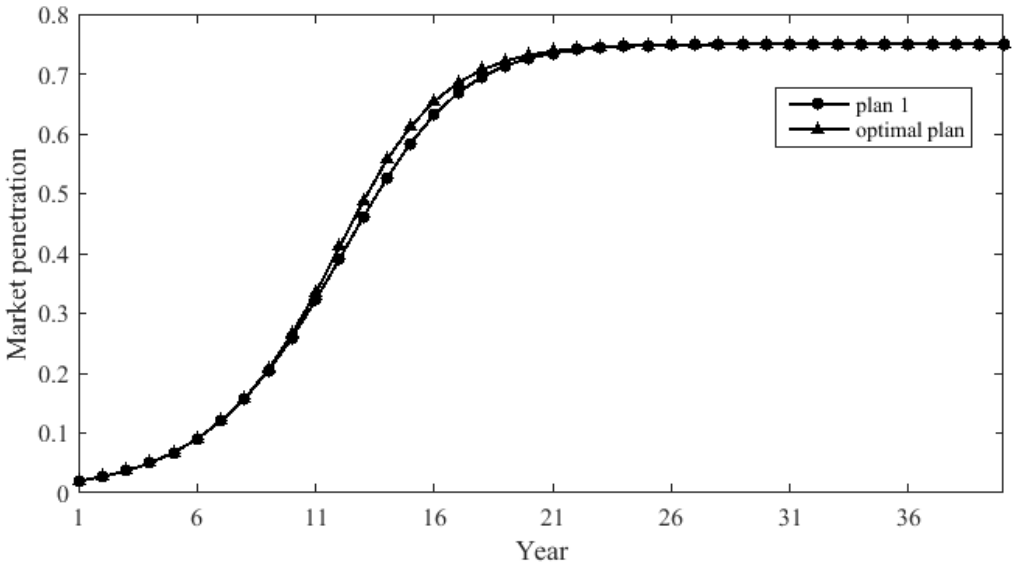

Figure 2-11. Evolution of AV market penetration under plan 1 and the optimal plan

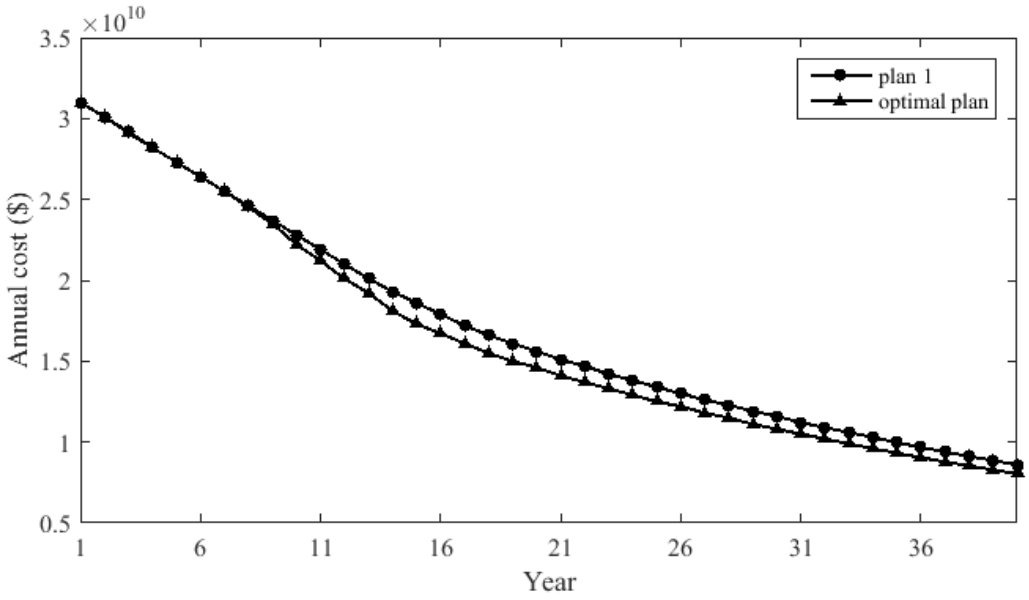

Figure 2-12. Evolution of annual cost under plan 1 and the optimal plan

CHAPTER 3 OPTIMAL DESIGN OF AUTONOMOUS VEHICLE ZONES IN TRANSPORTATION NETWORKS

In this chapter, Section 3.1 illustrates the operational concept of AV zones considered in this chapter and basic assumptions for the proposed models. Section 3.2 formulates the mixed routing equilibrium model and proposes its solution algorithm. Further, Section 3.3 optimizes the design of AV zones.

For convenient, we redefine the notations, and below are the ones frequently used in this chapter.

Sets	
N	Set of regular nodes
A	Set of regular links
$\widetilde{N}$	Set of AV nodes
$\tilde{A}$	Set of AV links
$\widehat{N}$	Set of dummy AV nodes
$\hat{A}$	Set of dummy AV links
W	Set of origin-destination (O-D) pairs
$\widetilde{W}$	Set of entrance-exit (E-E) pairs for the AV zone/network
M	Set of modes or classes, including CVs and AVs
$P^{w,m}$	Set of paths between O-D pair $w \in W$ by mode $m \in M$

$A(p)$	Set of links along path $p \in P^{w,m}$ between O-D pair $w \in W$ by mode $m \in M$
Parameters	
a	Link $a = (i,j) \in A \cup \hat{A}$ on the revised network
$\tilde{a}$	Link $\tilde{a} = (i,j) \in \tilde{A}$ on the AV network
w	O-D pair $w \in W$
$\tilde{w}$	E-E pair $\tilde{w} \in \tilde{W}$
m	Mode $m \in M$
$d^{w,m}$	Travel demand between O-D pair $w \in W$ by mode $m \in M$
$o(\tilde{w})$	Entrance of E-E pair $\tilde{w} \in \tilde{W}$
$d(\tilde{w})$	Exit of E-E pair $\tilde{w} \in \tilde{W}$
p	Path $p \in P^{w,m}$ between O-D pair $w \in W$ by mode $m \in M$
Variables	
v_a	Traffic flow of link $a \in A \cup \hat{A}$
$v_{\tilde{a}}$	Traffic flow of link $\tilde{a} \in \tilde{A}$
$x_a^{w,m}$	Link flow on link $a \in A \cup \hat{A}$ for O-D pair $w \in W$ by mode $m \in M$
$x_{\tilde{a}}^{\tilde{w}}$	Link flow on link $\tilde{a} \in \tilde{A}$ for E-E pair $\tilde{w} \in \tilde{W}$
$t_a(v_a)$	Travel time of link $a \in A$ specified by the link performance function
$t_{\tilde{a}}(v_{\tilde{a}})$	Travel time of link $\tilde{a} \in \tilde{A}$ specified by the link performance function
c_a	Travel time of dummy AV link $a \in \hat{A}$

3.1 PROBLEM DESCRIPTION

We consider a network where both AVs and CVs are present. The origin-destination (O-D) matrices of the vehicular trips of AVs and CVs are considered given. It is envisioned that a government agency strategically designs AV zones on a road network. An AV zone is cordoned off by a virtual loop. See Figure 3-1 for an example of where the nodes and links within loop C comprise an AV zone. To facilitate the presentation of the model formulation, this chapter hereinafter considers the deployment or presence of a single AV zone over the network, but the proposed model can be easily extended to the case with multiple AV zones directly. Below we illustrate the operational concept for the AV zone:

i. Only AVs are allowed to use the links within the zone;
ii. When entering the zone, AVs must report their exits of the zone to the control center, which routes AVs to traverse the zone;
iii. Based on AVs' entrances and exits, the control center routes AVs to minimize the total travel time in the zone.

In the presence of an AV zone, when making their route choices, CVs need to avoid the zone while AVs will decide whether to access the zone, and where to enter and exit. Note that among all paths connecting the same O-D pair, some may traverse the AV zone while others will

not. When comparing these paths, AVs need to perceive the times spent within and outside of the AV zone.

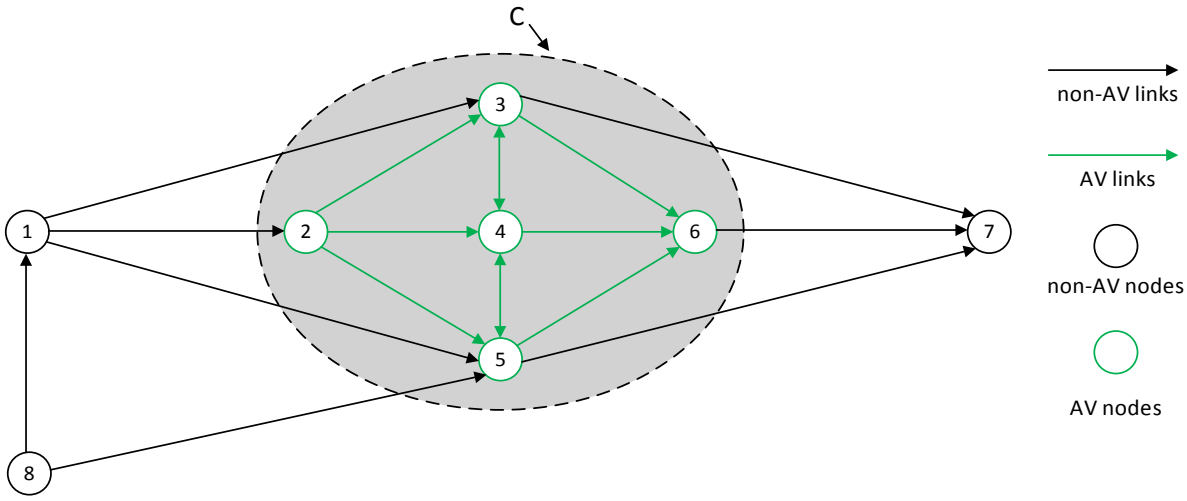

Figure 3-1. An example of AV zone

Since the overarching goal of this chapter is AV zone planning, a static deterministic modeling framework is adopted. Below we summarize basic assumptions for our model formulations:

i. AVs using the same entrance and exit of the AV zone may experience different travel times due to system-optimum routing. We assume that AVs perceive their travel times to be the minimum travel times between their corresponding entrances and exits of the AV zone.
ii. All vehicles are assumed to minimize their own trip times.
iii. The per-lane capacity of links within the AV zone is much larger than those of regular links due to vehicle automation.
iv. The capacity of a regular link with mixed traffic of CVs and AVs remains the same as when only CVs use the link.
v. The performance functions of regular and AV links may be different, but all are increasing functions with link flows.
vi. In the network equilibrium model, there exists at least one usable path between each O-D pair for both AVs and CVs. When designing the AV zone, if certain inner nodes within the zone are origins or destinations, the corresponding demands of CVs will be discarded for equilibrium analysis, because no feasible path will exist for CVs between these O-D pairs. Subsequently, the resulting loss of social welfare will be calculated as part of the social cost, which is the objective that government agencies aim at minimizing.

It is worth noting here that the equilibrium model developed in this chapter is different from previous network equilibrium analyses of AV flows, e.g., Correia and van Arem (2016), which focus on shared-use automated mobility and explicitly consider automated vehicle routing

to meet the travel demands of households; all households act selfishly in choosing their paths and schedules. In contrast, this chapter assumes that the vehicular O-D pattern of AVs is known and focuses on modeling the mixed routing behaviors that arise with the existence of AV zones.

3.2 MIXED ROUTING EQUILIBRIUM MODEL

Let $\tilde{G}(\tilde{N}, \tilde{A})$ denote the network within the AV zone, where $\tilde{N}$ and $\tilde{A}$ are the sets of nodes and links in the zone, respectively. For convenience, we hereinafter refer to them as AV network, AV nodes, and AV links. Based on $\tilde{G}(\tilde{N}, \tilde{A})$, we construct a dummy AV network to replace the original AV network. Specifically, such a dummy AV network only consists of those AV nodes that are either entrances or exits of the AV zone (e.g., nodes 2, 3, 5, and 6 in Figure 3-1, and we hereinafter refer to them as dummy AV nodes). Moreover, if an AV node is either an origin or a destination, it will also be regarded as an entrance or an exit of the AV zone. Further, dummy AV links are constructed to specify the connectivity between those nodes. For example, for the AV zone in Figure 3-1, if node 4 is neither an origin nor a destination, then the dummy AV links can be constructed as Figure 3-2(a); otherwise, Figure 3-2(b). By doing so, each dummy AV link represents a set of paths connecting an entrance and an exit. For example, dummy AV link 2-3 in Figure 3-2(a) represents paths $2 \rightarrow 3$, $2 \rightarrow 4 \rightarrow 3$, and $2 \rightarrow 5 \rightarrow 4 \rightarrow 3$ in Figure 3-1. Consequently, the flow on dummy link 2-3 represents the demand between entrance 2 and exit 3. In addition, as per Assumption i in Section 2, its travel time is equal to the shortest time of paths $2 \rightarrow 3$, $2 \rightarrow 4 \rightarrow 3$, and $2 \rightarrow 5 \rightarrow 4 \rightarrow 3$ in Figure 3-1. In other words, a dummy AV link can be viewed as the shortest path connecting the associated entrance and exit. Let $\hat{G}(\hat{N}, \hat{A})$ denote the dummy AV network where $\hat{N}$ and $\hat{A}$ are the sets of dummy AV nodes and links.

Let N and A denote the sets of non-AV or regular nodes and non-AV or regular links that are nodes and links outside of the AV zone (e.g., nodes 1, 7, and links 1-3, 8-1 in Figure 3-1). Let $G(N \cup \hat{N}, A \cup \hat{A})$ denote the network containing non-AV nodes, non-AV links, and dummy AV nodes and links (we refer to G as a revised network). For example, if node 4 is neither an origin nor a destination, then Figure 3-3 illustrates the revised network. In a revised network, we only need to consider the user-optimum routing principle without worrying about the mixed routing behaviors that exist in the original network.

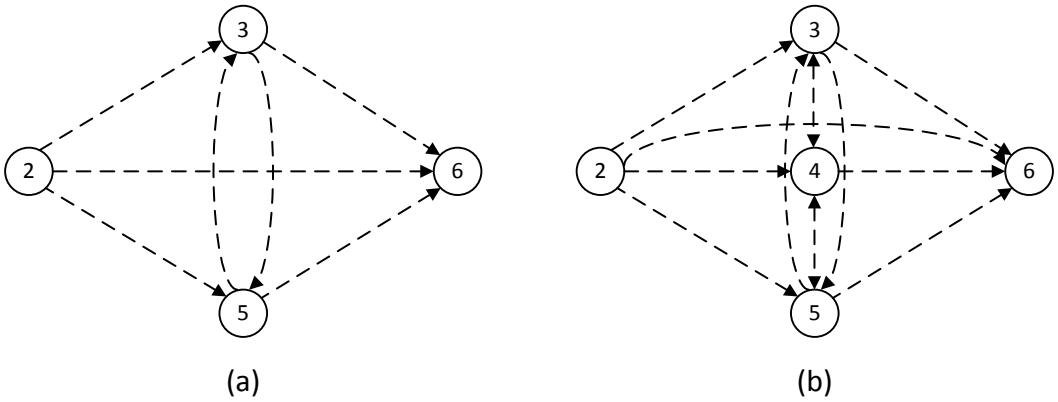

Figure 3-2. Dummy AV networks

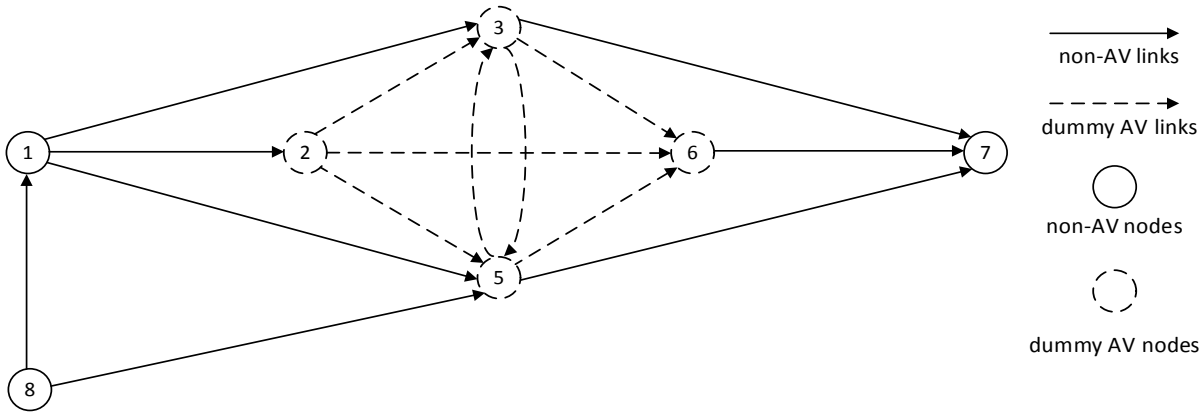

Figure 3-3. A revised network

We represent a link in the revised network as $a \in A \cup \hat{A}$, or its starting and ending nodes, i.e., $a = (i, j) \in A \cup \hat{A}$. Similarly, $\tilde{a} \in \tilde{A}$ represents an AV link. Let W and $\widetilde{W}$ denote the sets of O-D pairs for the revised network (note that these O-D pairs are the same as those in the original network), and entrance-exit (E-E) pairs associated with the AV network. Further, we use $o(\tilde{w})$ and $d(\tilde{w})$ to denote the entrance and exit of E-E pair $\tilde{w} \in \widetilde{W}$. Let M be the set of transportation modes CVs and AVs, i.e., $M = \{C, A\}$. Let $d^{w,m}$ and $P^{w,m}$ represent the travel demand and the set of paths between O-D pair $w \in W$ by mode $m \in M$, respectively. Let $x_a^{w,m}$ be the flow on link $a \in A \cup \hat{A}$ for O-D pair $w \in W$ by mode $m \in M$, and $x_{\tilde{a}}^{\tilde{w}}$ be the flow on link $\tilde{a} \in \tilde{A}$ for E-E pair $\tilde{w} \in \widetilde{W}$. Let v_a and $v_{\tilde{a}}$ be the aggregate flows of links $a \in A \cup \hat{A}$ and $\tilde{a} \in \tilde{A}$. Let $t_a(v_a)$ and $t_{\tilde{a}}(v_{\tilde{a}})$ define the travel times of links $a \in A$ and $\tilde{a} \in \tilde{A}$ specified by the performance functions of the links. Note that, according to Assumption iii, the per-lane capacity of each link within the AV zone, i.e., $\tilde{a} \in \tilde{A}$, will be substantially improved. Let c_a represent the travel time of dummy AV link $a \in \hat{A}$.

3.2.1 Travel Time of Dummy Links

As previously mentioned, c_a is assumed to be equal to the minimum trip time of the corresponding E-E pair $\tilde{w} \in \widetilde{W}$. Specifically, with a given traffic flow distribution of the AV network, $v_{\tilde{a}}, \forall \tilde{a} \in \tilde{A}$, finding the shortest path can be formulated as follows for each E-E pair $\tilde{w} \in \widetilde{W}$:

SP:

$$\min_{\mathbf{z}} \sum_{\tilde{a} \in \tilde{A}} t_{\tilde{a}}(v_{\tilde{a}}) z_{\tilde{a}}^{\tilde{w}}$$

$$\text{s.t. } \tilde{\Delta} \boldsymbol{z}^{\tilde{w}} = \tilde{E}^{\tilde{w}} \tag{3-1}$$

$$z_{\tilde{a}}^{\tilde{w}} \geq 0 \qquad \forall \tilde{a} \in \tilde{A} \tag{3-2}$$

where $\tilde{\Delta}$ is the node-link incidence matrix associated with the AV network and $\tilde{E}^{\tilde{w}}$ is a vector with a length of $|\tilde{N}|$. The vector consists of two-nonzero components: one has a value of 1 in the

component corresponding to the entrance of $\widetilde{w} \in \widetilde{W}$, and the other has a value of -1 in the component corresponding to the exit of $\widetilde{w} \in \widetilde{W}$.

In the above, the objective function is to minimize the total trip time. Constraint (3-1) ensures flow balance, and constraint (3-2) makes sure that $\boldsymbol{z}$ are nonnegative variables. Since the matrix associated with constraint (3-1) is totally unimodular, the optimal solution of SP must be integers. Further, based on constraint (3-1) and the objective function, it is easy to verify that the optimal value of $\boldsymbol{z}$ cannot be greater than 1. Therefore, the optimal solution $z_{\tilde{a}}^{\widetilde{w}*}, \forall \tilde{a} \in \tilde{A}$, is equal to either 0 or 1. Specifically, $z_{\tilde{a}}^{\widetilde{w}*} = 1$ if link $\tilde{a}$ is utilized, and 0 otherwise. Therefore, we can obtain the travel time of dummy AV link $a \in \hat{A}$ as below:

$$c_a = \sum_{\widetilde{w} \in \widetilde{W}} \beta_a^{\widetilde{w}} \left[\sum_{\tilde{a} \in \tilde{A}} t_{\tilde{a}}(v_{\tilde{a}}) z_{\tilde{a}}^{\widetilde{w}*} \right] \tag{3-3}$$

where $\beta_a^{\widetilde{w}}$ is a binary parameter that equals 1 if the dummy link a corresponds to the E-E pair $\widetilde{w} \in \widetilde{W}$, and 0 otherwise.

SP is a linear program written for each E-E pair $\widetilde{w} \in \widetilde{W}$. Its optimality conditions are stated as follows:

(3-1)-(3-2)

$$\left[t_{\tilde{a}}(v_{\tilde{a}}) - \kappa_i^{\widetilde{w}} + \kappa_j^{\widetilde{w}}\right] z_{\tilde{a}}^{\widetilde{w}} = 0 \qquad \forall \tilde{a} = (i,j) \in \tilde{A}, \widetilde{w} \in \widetilde{W} \tag{3-4}$$

$$t_{\tilde{a}}(v_{\tilde{a}}) - \kappa_i^{\widetilde{w}} + \kappa_j^{\widetilde{w}} \geq 0 \qquad \forall \tilde{a} = (i,j) \in \tilde{A}, \widetilde{w} \in \widetilde{W} \tag{3-5}$$

where $\boldsymbol{\kappa}$ are the multipliers associated with constraints (3-1).

3.2.2 User Equilibrium Flow Distribution in the Revised Network

As previously mentioned, in the revised network, we only need to consider the user-optimum routing principle. With c_a calculated as above for $a \in \hat{A}$, the user equilibrium conditions can be mathematically defined as follows:

$$\boldsymbol{\Delta x}^{w,m} = \boldsymbol{E}^{w,m} d^{w,m} \qquad \forall m \in M, w \in W \tag{3-6}$$

$$x_a^{w,A} \geq 0 \qquad \forall a \in A \cup \hat{A}, w \in W \tag{3-7}$$

$$x_a^{w,C} \geq 0 \qquad \forall a \in A, w \in W \tag{3-8}$$

$$x_a^{w,C} = 0 \qquad \forall a \in \hat{A}, w \in W \tag{3-9}$$

$$v_a = \sum_{w \in W} \sum_{m \in M} x_a^{w,m} \qquad \forall a \in A \cup \hat{A} \tag{3-10}$$

$$t_a(v_a) - \rho_i^{w,m} + \rho_j^{w,m} \geq 0 \qquad \forall a = (i,j) \in A, w \in W, m \in M \tag{3-11}$$

$$c_a(v_a) - \rho_i^{w,A} + \rho_j^{w,A} \geq 0 \qquad \forall a = (i,j) \in \hat{A}, w \in W \tag{3-12}$$

$$\left(t_a(v_a) - \rho_i^{w,m} + \rho_j^{w,m}\right) \cdot x_a^{w,m} = 0 \qquad \forall a = (i,j) \in A, w \in W, m \in M \qquad (3\text{-}13)$$

$$\left(c_a(v_a) - \rho_i^{w,A} + \rho_j^{w,A}\right) \cdot x_a^{w,A} = 0 \qquad \forall a = (i,j) \in \hat{A}, w \in W \qquad (3\text{-}14)$$

where Δ is the node-link incidence matrix associated with the revised network and E^w is a vector with a length of $|N|$. The vector consists of two-nonzero components: one has a value of 1 in the component corresponding to the origin of $w \in W$, and the other has a value of -1 in the component corresponding to the destination of $w \in W$. $\boldsymbol{\rho}$ are auxiliary variables representing the node potentials.

In the above, constraint (3-6) ensures flow balance. Constraints (3-7) and (3-8) imply that the link flow between each O-D pair by each mode should be nonnegative, and constraint (3-9) ensures that only AVs can use dummy AV links. Constraint (3-10) implies that the aggregate link flow is the summation of link flow between different O-D pairs by different modes. Constraints (3-11)-(3-14) are complementary slackness conditions, ensuring that the perceived travel times of utilized paths between an O-D pair for the same mode are the same, but less than or equal to that of any unutilized usable path. Specifically, a path is usable for a mode if all the links along the path are usable for the mode. For example, a path containing any AV link is not usable for CVs.

3.2.3 System-Optimum Routing within the AV Network

As mentioned before, the demand for each E-E pair equals the flow of the corresponding dummy AV link. Specifically, given the flow distribution of the revised network, the flow of a dummy AV link, say $\ddot{a} \in \hat{A}$, is calculated to be $\sum_{w \in W} x_{\ddot{a}}^{w,A}$. Therefore, the system-optimum flow distribution within the AV zone can be formulated as follows:

$$\sum_j x_{o(\tilde{w}),j}^{\tilde{w}} - \sum_k x_{k,o(\tilde{w})}^{\tilde{w}} = \sum_{a \in \hat{A}} \beta_a^{\tilde{w}} \sum_{w \in W} x_a^{w,A} \qquad \forall \tilde{w} \in \tilde{W} \qquad (3\text{-}15)$$

$$\sum_j x_{d(\tilde{w}),j}^{\tilde{w}} - \sum_k x_{k,d(\tilde{w})}^{\tilde{w}} = -\sum_{a \in \hat{A}} \beta_a^{\tilde{w}} \sum_{w \in W} x_a^{w,A} \qquad \forall \tilde{w} \in \tilde{W} \qquad (3\text{-}16)$$

$$\sum_j x_{i,j}^{\tilde{w}} - \sum_k x_{k,i}^{\tilde{w}} = 0 \qquad \forall i \in \tilde{N} \backslash \{o(\tilde{w}), d(\tilde{w})\}, \tilde{w} \in \tilde{W} \qquad (3\text{-}17)$$

$$x_{\tilde{a}}^{\tilde{w}} \geq 0 \qquad \forall \tilde{a} \in \tilde{A}, \tilde{w} \in \tilde{W} \qquad (3\text{-}18)$$

$$v_{\tilde{a}} = \sum_{\tilde{w} \in \tilde{W}} x_{\tilde{a}}^{\tilde{w}} \qquad \forall \tilde{a} \in \tilde{A} \qquad (3\text{-}19)$$

$$t_{\tilde{a}}(v_{\tilde{a}}) + v_{\tilde{a}} t'_{\tilde{a}}(v_{\tilde{a}}) - \tilde{\rho}_i^{\tilde{w}} + \tilde{\rho}_j^{\tilde{w}} \geq 0 \qquad \forall \tilde{a} \in \tilde{A}, \tilde{w} \in \tilde{W} \qquad (3\text{-}20)$$

$$\left(t_{\tilde{a}}(v_{\tilde{a}}) + v_{\tilde{a}} t'_{\tilde{a}}(v_{\tilde{a}}) - \tilde{\rho}_i^{\tilde{w}} + \tilde{\rho}_j^{\tilde{w}}\right) \cdot x_{\tilde{a}}^{\tilde{w}} = 0 \qquad \forall \tilde{a} \in \tilde{A}, \tilde{w} \in \tilde{W} \qquad (3\text{-}21)$$

where $\tilde{\boldsymbol{\rho}}$ are auxiliary variables, representing the node potentials.

In the above, constraints (3-15)-(3-17) ensure flow balance. Constraint (3-18) suggests that the link flow of each E-E pair is nonnegative. Constraint (3-19) implies that the AV link flow is the summation of link flow for different E-E pairs. Constraints (3-20) and (3-21) are complementary slackness conditions, specifying that marginal travel times of utilized paths between an E-E pair are the same, but less than or equal to that of any unutilized path.

3.2.4 Mixed Routing Equilibrium

Definition 1. At the mixed routing equilibrium, for the same mode, perceived travel times of utilized paths between an O-D pair are the same, but less than or equal to that of any unutilized usable path between the same O-D pair.

In the above definition, perceived travel times for CVs are their actual trip times, while the ones for AVs are the actual travel time spent outside of the AV zone, plus the perceived travel times spent within the zone. Recall that the latter is equivalent to the minimum travel time between AVs' corresponding entrances and exits of the AV zone (see Assumption i).

Mathematically, we can define the mixed routing equilibrium conditions (MRE) for the original network as (3-1)-(3-21). Specifically, (3-6)-(3-14) specify that, given the perceived travel times within the AV zone, the flow distribution must satisfy the network equilibrium conditions for the revised network; (3-1)-(3-5) ensure that AVs' perceived travel times within the AV zone equal the minimum travel times between their corresponding entrances and exits of the zone; (3-15)-(3-21) imply that, within the AV zone, AVs must follow the system-optimum routing principle.

To further formulate an equivalent mixed routing equilibrium model, we define a set $\Lambda = \{(\boldsymbol{v}, \boldsymbol{x}, \tilde{\boldsymbol{\rho}}, \boldsymbol{z}, \boldsymbol{\tau})\}$, where the vector satisfies the following conditions:

(3-1), (3-2), (3-6)-(3-10), (3-18), (3-19)

$$\tilde{\rho}_i^{\tilde{w}} \geq 0 \qquad \forall i \in \tilde{N}, \tilde{w} \in \tilde{W} \qquad (3\text{-}22)$$

$$\tau_i^{\tilde{w}} \geq 0 \qquad \forall i \in \tilde{N} \backslash d(\tilde{w}), \tilde{w} \in \tilde{W} \qquad (3\text{-}23)$$

where $\boldsymbol{\tau}$ are auxiliary variables introduced to facilitate formulating the problem as follows.

Proposition 1. The mixed routing equilibrium conditions (3-1)-(3-21) are equivalent to finding $(\boldsymbol{v}^*, \boldsymbol{x}^*, \tilde{\boldsymbol{\rho}}^*, \boldsymbol{z}^*, \boldsymbol{\tau}^*) \in \Lambda$, which solves the following variational inequality:

MRE-VI:

$$\sum_{a\in A} t_a(v_a^*)(v_a - v_a^*) + \sum_{a\in \hat{A}}\Big[\sum_{\tilde{w}\in\tilde{W}} \beta_a^{\tilde{w}} \sum_{\tilde{a}\in\tilde{A}} t_{\tilde{a}}(v_{\tilde{a}}^*) z_{\tilde{a}}^{\tilde{w}^*}\Big](v_a - v_a^*) + \sum_{\tilde{w}} \sum_{\tilde{a}\in\tilde{A}}\Big[t_{\tilde{a}}(v_{\tilde{a}}^*) + v_{\tilde{a}}^* t'_{\tilde{a}}(v_{\tilde{a}}^*) - \big(\tilde{\rho}_i^{\tilde{w}*} - \tilde{\rho}_j^{\tilde{w}*}\big)\Big]\big(x_{\tilde{a}}^{\tilde{w}} - x_{\tilde{a}}^{\tilde{w}*}\big) + \sum_{\tilde{w}}\Big[\Big(\sum_j x_{o(\tilde{w}),j}^{\tilde{w}*} - \sum_k x_{k,o(\tilde{w})}^{\tilde{w}*}\Big) - \sum_{a\in\hat{A}} \beta_a^{\tilde{w}} \sum_{w\in W} x_a^{w,A*}\Big]\big(\tilde{\rho}_{o(\tilde{w})}^{\tilde{w}} - \tilde{\rho}_{o(\tilde{w})}^{\tilde{w}*}\big) - \sum_{\tilde{w}}\Big[\Big(\sum_j x_{o(\tilde{w}),j}^{\tilde{w}*} - \sum_k x_{k,o(\tilde{w})}^{\tilde{w}*}\Big) - \sum_{a\in\hat{A}} \beta_a^{\tilde{w}} \sum_{w\in W} x_a^{w,A*}\Big]\big(\tau_{o(\tilde{w})}^{\tilde{w}} - \tau_{o(\tilde{w})}^{\tilde{w}*}\big) + \sum_{\tilde{w}} \sum_{i\in\tilde{N}\backslash\{o(\tilde{w}),d(\tilde{w})\}}\Big(\sum_j x_{i,j}^{\tilde{w}*} - \sum_k x_{k,i}^{\tilde{w}*}\Big)\big(\tilde{\rho}_i^{\tilde{w}} - \tilde{\rho}_i^{\tilde{w}*}\big) -$$

$\sum_{\tilde{w}} \sum_{i \in \tilde{N} \setminus \{o(\tilde{w}), d(\tilde{w})\}} \left(\sum_j x_{i,j}^{\tilde{w}*} - \sum_k x_{k,i}^{\tilde{w}*} \right) \left(\tau_i^{\tilde{w}} - \tau_i^{\tilde{w}*} \right) + \sum_{\tilde{w}} \sum_{\tilde{a} \in \tilde{A}} t_{\tilde{a}}(v_{\tilde{a}}^*) \left(z_{\tilde{a}}^{\tilde{w}} - z_{\tilde{a}}^{\tilde{w}*} \right) \geq 0, \forall (\boldsymbol{v}, \boldsymbol{x}, \tilde{\boldsymbol{\rho}}, \boldsymbol{z}, \boldsymbol{\tau}) \in \Lambda$

The equivalence can be established by expressing the optimality conditions of MRE-VI and comparing them with the defined mixed routing equilibrium conditions, i.e., MRE. See the appendix for a proof.

Proposition 2. MRE-VI has at least one solution.

Proof: According to the appendix, we know that $\boldsymbol{\tau}$ are nonnegative auxiliary variables that are only used to guarantee the flow balance within the AV network, i.e., (A.44), (A.47), and (A.48); thus, adding some upper bounds to $\boldsymbol{\tau}$ will not affect the other optimal solutions $(\boldsymbol{v}^*, \boldsymbol{x}^*, \tilde{\boldsymbol{\rho}}^*, \boldsymbol{z}^*)$. Furthermore, since $\tilde{\boldsymbol{\rho}}$ represent node potentials, we can always find some upper bounds for them, within which optimal values of these multipliers still exist. As a result, we can construct a restricted MRE-VI by adding corresponding upper bounds to $(\tilde{\boldsymbol{\rho}}, \boldsymbol{\tau})$**.** In addition, link flows $\boldsymbol{x}$ and $\boldsymbol{v}$ are bounded, and the upper bound of $\boldsymbol{z}$ is $\mathbf{1}$, which has been demonstrated in Section 3.1. Therefore, the restricted MRE-VI problem has a compact and convex feasible region. Given that all the functions are continuous, the restricted MRE-VI admits at least one solution (see, e.g., Harker and Pang, 1990), so as the original MRE-VI. □

However, even if all the link performance functions of both the regular and AV links are strictly monotone, we cannot guarantee the uniqueness of the link flow solution to MRE-VI, as the travel time functions of dummy links (see equality (3-3)) may not be strictly monotone with respect to the link flows in the revised network.

To illustrate, we consider a simple AV network shown in Figure 3-4(a). The link travel time functions are assumed to be: $t_{12}(x_{12}) = 3x_{12}$, $t_{13}(x_{13}) = 3x_{13}$, and $t_{23}(x_{23}) = 3x_{23}$, where x_{12}, x_{13}, and x_{23} are the corresponding link flows. Suppose that 1-2, 1-3, and 2-3 are E-E pairs, then the dummy network is constructed as the same as the original AV network (see Figure 3-4(b)). It is worth pointing out that dummy link 1-3 represents the shorter path of path $1 \rightarrow 3$ and path $1 \rightarrow 2 \rightarrow 3$. Let e_{12}, e_{13}, and e_{23} denote the dummy flows of link 1-2, 1-3, and 2-3, i.e., the demand of E-E pair 1-2, 1-3, and 2-3, respectively. Furthermore, we assume that $e_{13} > e_{12} + e_{23}$. It is easy to verify that under this assumption, both paths $1 \rightarrow 3$ and $1 \rightarrow 2 \rightarrow 3$ of the AV network will be utilized by the trips from E-E pair 1-3. Define the trips using path $1 \rightarrow 2 \rightarrow 3$ as $\hat{e}_{13}$, then the ones using path $1 \rightarrow 3$ are $e_{13} - \hat{e}_{13}$. As a result, we have $x_{12} = e_{12} + \hat{e}_{13}$, $x_{13} = e_{13} - \hat{e}_{13}$, and $x_{23} = e_{23} + \hat{e}_{13}$. According to the system-optimum routing principle, the marginal cost of path $1 \rightarrow 3$ and $1 \rightarrow 2 \rightarrow 3$ must be equivalent. That is,

$$6(e_{13} - \hat{e}_{13}) = 6(e_{12} + \hat{e}_{13}) + 6(e_{23} + \hat{e}_{13})$$

which yields $\hat{e}_{13} = \frac{1}{3}(e_{13} - e_{12} - e_{23})$.

Based on the flow distribution, we can obtain the travel time functions of the dummy links: $c_{12} = t_{12}(x_{12}) = 2e_{12} + e_{13} - e_{23}$, $c_{13} = t_{13}(x_{13}) = 2e_{13} + e_{12} + e_{23}$, and $c_{23} = t_{23}(x_{23}) = 2e_{23} + e_{13} - e_{12}$. It is easy to verify that the Jacobian matrix of $\boldsymbol{c}$ with respect to $\boldsymbol{e}$ is only positive semi-definite, rather than positive definite. That is, the travel time functions of

dummy links are not strictly monotone with respect to the link flows in the revised network. Consequently, the link flow solution to MRE-VI may not be unique.

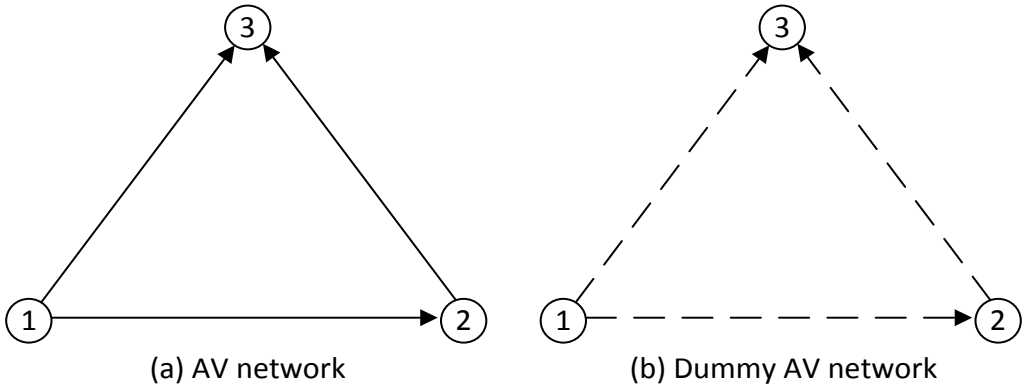

Figure 3-4. A simple AV network and its corresponding dummy network

3.2.5 Solution Procedure

In this section, we solve MRE-VI by reformulating it to be the following nonlinear optimization problem via a technique proposed by Aghassi et al. (2006):

MRE-NLP:

$$\min_{\boldsymbol{v},\boldsymbol{x},\tilde{\boldsymbol{p}},\boldsymbol{z},\tilde{\boldsymbol{\alpha}},\tilde{\boldsymbol{\beta}},\tilde{\boldsymbol{\lambda}},\tilde{\boldsymbol{\gamma}}} \sum_{a\in A} t_a(v_a)v_a + \sum_{a\in\hat{A}} c_a(v_a)v_a + \sum_{\tilde{w}\in\tilde{W}}\sum_{\tilde{a}\in\tilde{A}}\left[t_{\tilde{a}}(v_{\tilde{a}}) + v_{\tilde{a}}t'_{\tilde{a}}(v_{\tilde{a}}) - \left(\tilde{\rho}_i^{\tilde{w}} - \tilde{\rho}_j^{\tilde{w}}\right)\right]x_{\tilde{a}}^{\tilde{w}} - \sum_{w\in W}\sum_{m\in M}\sum_{i\in N} d_i^{w,m}\tilde{\alpha}_i^{w,m} - \sum_{\tilde{w}\in\tilde{W}}\left(\tilde{\gamma}_{o(\tilde{w})}^{\tilde{w}} - \tilde{\gamma}_{d(\tilde{w})}^{\tilde{w}}\right)$$

s.t. (3-1), (3-2), (3-6)-(3-10), (3-18), (3-19), and (3-22)

$$\tilde{\beta}_a = t_a(v_a) \qquad \forall a \in A$$

$$\tilde{\beta}_a = \sum_{\tilde{w}\in\tilde{W}} \beta_a^{\tilde{w}} \sum_{\tilde{a}\in\tilde{A}} t_{\tilde{a}}(v_{\tilde{a}})z_{\tilde{a}}^{\tilde{w}} \qquad \forall a \in \hat{A}$$

$$\tilde{\lambda}_{\tilde{a}} = 0 \qquad \forall \tilde{a} \in \tilde{A}$$

$$\tilde{\alpha}_i^{w,A} - \tilde{\alpha}_j^{w,A} - \tilde{\beta}_a \le 0 \qquad \forall a \in A \cup \hat{A}, w \in W$$

$$\tilde{\alpha}_i^{w,C} - \tilde{\alpha}_j^{w,C} - \tilde{\beta}_a \le 0 \qquad \forall a \in A, w \in W$$

$$-\tilde{\lambda}_{\tilde{a}} \le t_{\tilde{a}}(v_{\tilde{a}}) + v_{\tilde{a}}t'_{\tilde{a}}(v_{\tilde{a}}) - \tilde{\rho}_i^{\tilde{w}} + \tilde{\rho}_j^{\tilde{w}} \qquad \forall \tilde{a} \in \tilde{A}, \tilde{w} \in \tilde{W}$$

$$\left(\sum_j x_{o(\tilde{w}),j}^{\tilde{w}} - \sum_k x_{k,o(\tilde{w})}^{\tilde{w}}\right) - \sum_{a\in\hat{A}} \beta_a^{\tilde{w}} \sum_{w\in W} x_a^{w,A} = 0 \qquad \forall \tilde{w} \in \tilde{W}$$

$$\sum_j x_{i,j}^{\tilde{w}} - \sum_k x_{k,i}^{\tilde{w}} = 0 \qquad \forall i \in \tilde{N}\backslash\{o(\tilde{w}), d(\tilde{w})\}, \tilde{w} \in \tilde{W}$$

$$\tilde{\gamma}_i^{\tilde{w}} - \tilde{\gamma}_j^{\tilde{w}} \le t_{\tilde{a}}(v_{\tilde{a}}) \qquad \forall \tilde{a} \in \tilde{A}, \tilde{w} \in \tilde{W}$$

where $\tilde{\alpha}_i^{w,A}$, $\tilde{\alpha}_i^{w,C}$, $\tilde{\beta}_a$, $\tilde{\lambda}_{\tilde{a}}$, and $\tilde{\gamma}_i^{\tilde{w}}$ are auxiliary variables, and $d_i^{w,m} = d^{w,m}$, if $i = o(w)$; $d_i^{w,m} = -d^{w,m}$, if $i = d(w)$; otherwise, $d_i^{w,m} = 0$.

Specifically, if the optimal value of MRE-NLP is 0, then its solution $(\boldsymbol{v}^*, \boldsymbol{x}^*, \tilde{\boldsymbol{\rho}}^*, \boldsymbol{z}^*, \boldsymbol{\tau}^*)$ is also the one to MRE-VI.

3.2.6 Numerical Example

In this section, numerical examples are conducted based on the network in Figure 3-1. Specifically, there are two O-D pairs with demands shown in Table 3-1, and the link performance function is assumed to be $t_a(v_a) = a_0 + b_0 \times v_a$ min, where a_0 and b_0 are provided in Table 3-2. We construct an AV zone as per Figure 3-1. That is, nodes 2, 3, 4, 5, and 6 are AV nodes. Accordingly, links 2-3, 2-4, 2-5, 3-4, 3-6, 4-3, 4-5, 4-6, 5-4, and 5-6 are all AV links. It is worthwhile to highlight that since node 4 is neither an origin nor a destination, the dummy network and revised network are constructed as Figure 3-2(a) and Figure 3-3, respectively. As per Assumption iii, we assume that the per-lane capacity becomes triple when a regular link is converted to an AV link. Hence, the AV link performance function is $t_{\tilde{a}}(v_{\tilde{a}}) = a_0 + \frac{b_0}{3} \times v_{\tilde{a}}$ min.

Table 3-1. O-D demand

O-D	CV	AV
1-7	40	30
8-7	25	15

Table 3-2. Network characteristics

Link	a_0 (min)	b_0	Link	a_0 (min)	b_0	Link	a_0 (min)	b_0
1-2	1.00	1.00	3-4	1.50	1.00	5-4	1.00	1.00
1-3	2.00	3.00	3-6	1.00	1.50	5-6	1.00	1.00
1-5	1.00	1.00	3-7	1.00	1.00	5-7	2.00	2.00
2-3	2.00	1.00	4-3	0.50	1.00	6-7	2.00	2.00
2-4	1.00	0.50	4-5	1.00	1.00	8-1	1.00	1.00
2-5	1.00	1.00	4-6	1.00	2.50	8-5	2.00	4.00

Given the above setting, we obtain the equilibrium solution by solving MRE-NLP. Specifically, Table 3-3 and Table 3-4 display the equilibrium link flows for the original network (see Figure 3-1) and the dummy network (see Figure 3-2(a)), respectively. As we can see, since CVs are not permitted to use the AV links, the equilibrium link flows on the AV links and dummy AV links are all 0. As mentioned previously, the demand for each E-E pair equals the flow of the corresponding dummy AV link. Therefore, the equilibrium link flows in Table 3-4 are also the E-E demand for the AV zone. Given the E-E demand, we obtain a system-optimum solution within the AV zone shown in Table 3-5 and Table 3-6. Comparing Table 3-3 with Table 3-5, it is easy to verify that the AV-link flows in Table 3-3 exactly follow the system-optimum flow distribution, which is consistent with the operation concept iii that AVs are routed to minimize the total travel time in the AV zone. Furthermore, making a comparison between Table 3-4 and Table 3-6, we can readily observe that the travel time of each dummy link in Table 3-4 is

equal to the minimum path travel time (i.e., the path travel times that are bold and underlined) of the corresponding E-E pair. For example, there are three paths 2 → 3, 2 → 4 → 3, and 2 → 5 → 4 → 3 between E-E pair 2-3, whose travel times are 7.16, 6.91, and 7.41 min, respectively (see Table 3-6). As expected, the travel time of dummy link 2-3 is 6.91 min (see Table 3-4), which equals the minimum of the three, i.e., 6.91.

Table 3-3. Equilibrium link flow for the original network

Link	CV flow	AV flow	Travel time (min)	Link	CV flow	AV flow	Travel time (min)
1-2	0.00	34.06	35.06	4-3	0.00	9.32	3.61
1-3	23.96	0.00	73.87	4-5	0.00	0.00	1.00
1-5	28.81	7.84	37.65	4-6	0.00	5.16	5.30
2-3	0.00	15.48	7.16	5-4	0.00	0.65	1.22
2-4	0.00	13.82	3.30	5-6	0.00	15.05	6.02
2-5	0.00	4.76	2.59	5-7	41.04	0.00	84.09
3-4	0.00	0.00	1.50	6-7	0.00	22.09	46.18
3-6	0.00	1.88	1.94	8-1	12.76	11.91	25.67
3-7	23.96	22.91	47.87	8-5	12.24	3.09	63.32

Table 3-4. Equilibrium link flow for the dummy network

Link	AV flow	Travel time (min)	Link	AV flow	Travel time (min)
2-3	22.91	6.91	3-6	0.00	1.94
2-5	0.32	2.59	5-3	0.00	4.82
2-6	10.83	8.60	5-6	11.25	6.02
3-5	0.00	2.50			

Table 3-5. System-optimum link flow pattern within the AV zone

Link	AV flow	Travel time (min)	Link	AV flow	Travel time (min)
2-3	15.48	7.16	4-3	9.32	3.61
2-4	13.82	3.30	4-5	0.00	1.00
2-5	4.76	2.59	4-6	5.16	5.30
3-4	0.00	1.50	5-4	0.65	1.22
3-6	1.88	1.94	5-6	15.05	6.02

Table 3-6. System-optimum path flow pattern within the AV zone

E-E	Path	Path flow	Path travel time (min)	Marginal path travel time (min)
2-3	2-3	13.60	7.16	12.32
	2-4-3	9.32	**6.91**	12.32
	2-5-4-3	0.00	7.41	12.32
2-5	2-5	0.32	**2.59**	4.17
	2-3-4-5	0.00	9.66	14.82
	2-4-5	0.00	4.30	6.61
2-6	2-3-4-6	0.00	13.96	23.42
	2-3-4-5-6	0.00	15.67	25.85
	2-3-6	1.88	9.10	15.20
	2-4-3-6	0.00	8.85	15.20
	2-4-5-6	0.00	10.32	17.64
	2-4-6	4.51	**8.60**	15.20
	2-5-4-3-6	0.00	9.35	15.20
	2-5-4-6	0.65	9.10	15.20
	2-5-6	3.79	**8.60**	15.20
3-5	3-4-5	0.00	**2.50**	2.50
3-6	3-4-5-6	0.00	8.52	13.53
	3-4-6	0.00	6.80	11.10
	3-6	0.00	**1.94**	2.88
5-3	5-4-3	0.00	**4.82**	8.15
5-6	5-4-3-6	0.00	6.77	11.03
	5-4-6	0.00	6.52	11.03
	5-6	11.25	**6.02**	11.03

Table 3-7 shows the perceived travel times of CVs and AVs with and without the AV zone. As we can see, without the AV zone, both CVs and AVs perceive the same travel time for the same O-D pair, as they share the same road network and link performance functions. However, with the AV zone deployed, the perceived travel times of AVs between both O-D pairs decrease substantially (e.g., by 19% between O-D pair 1-7), while the ones of CVs increase considerably (e.g., by 10% between O-D pair 1-7). This is due to the fact that the AV zone can be utilized only by AVs. Furthermore, as the per-lane capacity of links within the AV zone is assumed to be much larger than those of regular links due to vehicle automation (see Assumption iii), the total travel time with the AV zone is thus expected to be reduced. It can be seen from Table 3-8 that with the presence of the AV zone, the system travel time decreases from 13,202.75 min to 12,987.27 min. Besides the total system travel time, AV-zone planners may also want to analyze the impact of the AV zone on the AV-zone area (i.e., the area consisting of links 2-3, 2-4, 2-5, 3-4, 3-6, 4-3, 4-5, 4-6, 5-4, and 5-6). Table 3-8 shows that the total travel time within the AV-zone area decreases substantially, from 1,193.09 min to 324.69 min. The above

findings imply that deploying an AV zone may improve the performance of the AV-zone area as well as the whole system.

Table 3-7. Perceived travel times with and without the AV zone

Scenario	O-D	Perceived travel time of CV (min)	Perceived travel time of AV (min)
Without AV zone	1-7	110.88	110.88
	1-8	136.04	136.04
With AV zone	1-7	121.74	89.84
	1-8	147.40	115.51

Table 3-8. System and AV-zone area travel times with and without the AV zone

Scenario	System travel time (min)	Travel time within the AV-zone area (min)
Without AV zone	13,202.75	1,193.09
With AV zone	12,987.27	324.69

3.2.7 Discussions

The mixed routing equilibrium model discussed above may become more relevant with the deployment of various advanced traffic control and management strategies leveraging connected and automated vehicle technologies. The modeling framework proposed in this chapter can be applied to various scenarios where vehicles adopt different routing principles at different sub-networks, as long as the routing strategies and the perceived travel times within the sub-networks are well defined. Below is a detailed discussion:

- *Routing strategy within the sub-network*

As per the operation concept iii, the control center of the sub-network is assumed to route vehicles to minimize the total travel time in the sub-network. In practice, the control center may have different routing strategies for different sub-networks, such as minimizing vehicle-miles traveled or traffic emissions. The proposed model can be readily extended to consider variant routing strategies as long as the following conditions are satisfied:

i. The routing objective function is convex with respect to link flows within the sub-network.
ii. All constraints are linear.

With the above conditions being met, the routing problem within the sub-network is a convex problem and can be readily embedded into the mixed routing equilibrium model. More specifically, let ψ denote the optimality conditions of the convex problem, and then the mixed routing equilibrium conditions can be represented by $\{(1)-(14), \boldsymbol{y} \in \psi\}$, where $\boldsymbol{y}$ is the optimization variable vector. Consequently, the proposed model can be applied to multiple sub-networks with different routing strategies directly.

- *Perceived travel time within the sub-network*

According to Assumption i, the perceived travel times are assumed to be the minimum travel times between the corresponding entrances and exits of the sub-network, which implies an optimistic routing behavior. Other considerations can be accommodated; for example, the longest travel times (without loop) between the entrances and exits can be taken as the perceived travel times within the sub-network, which implies a pessimistic routing behavior. However, any consideration needs to ensure the perceived travel times to be uniquely defined. For example, the average travel time between an entrance and an exit appears a good proxy for the perceived travel time. Unfortunately, the value depends on the path flow distribution and may not be uniquely determined under the system-optimum routing principle. Consequently, taking it as the perceived travel time might lead to one driver having different perceived travel times even if the link flow distribution is given. In this situation, there may be an infinite number of network equilibrium flow patterns, which would impose a significant challenge for various planning applications that rely on the typically unique equilibrium flow distribution as the sole estimate or forecast of how traffic will react to changes in the transportation system. Additional care needs to be exercised to handle such situations (see, e.g., Lou et al., 2010; Ban et al., 2013; de Andrade et al., 2016).

3.3 OPTIMAL DESIGN OF AUTONOMOUS VEHICLE ZONE

Given the proposed mixed routing equilibrium model, we proceed to optimize the deployment plan of an AV zone over a general network. As previously stated, the problem can be formulated as a mixed-integer bi-level programming model. The lower-level problem is the mixed routing equilibrium model developed above, i.e., MRE-VI. In the upper-level problem, the decision variables specify where to set up the AV zone, i.e., which links are upgraded to be AV links. All AV links should be clustered and cordoned off by a virtual loop. When a link becomes an AV link, its per-lane capacity will be increased to a given value. The objective is to minimize the social cost, which consists of the construction cost, the total system travel time, and the loss of social welfare due to the loss of accessibility for some CV drivers. Mathematically, it is to minimize $\sum_{\tilde{a}\in\tilde{A}} s_{\tilde{a}} + \sum_{a\in A} t_a(v_a)v_a + \sum_{\tilde{a}\in\tilde{A}} t_{\tilde{a}}(v_{\tilde{a}})v_{\tilde{a}} + \sum_{w\in W} \varrho^w \zeta^w d^{w,C}$, where $s_{\tilde{a}}$ is the construction cost for AV link $\tilde{a}$; $\varrho^w = 1$, if the accessibility for O-D pair w is damaged by the presence of the AV zone, and 0 otherwise; ζ^w is the loss of benefit for a CV driver between O-D pair w due to the loss of accessibility.

3.3.1 Solution Procedure

Although the problem is NP-hard, a few heuristic algorithms can be applied to solve it effectively, such as those in Zhang and Yang (2004), Sumalee (2004), and Hult (2006). However, most of these existing heuristic algorithms may not generate new feasible design plans efficiently, with a few exceptions (e.g., Sumalee, 2004), where complicated strategies have been developed to ensure the feasibility of new design plans.

The simulated annealing algorithm or SAA is a probabilistic method proposed by Kirkpatrick et al. (1983) and Cerny (1985) for finding the global optimum of a given function. Its basic idea is to consider a neighboring solution of the current solution at each step, and apply a probability function to decide whether to move to the new solution or not. It stops until a maximum number of iterations is reached. This chapter applies SAA to solve the optimal design model, as an efficient procedure of finding new feasible design plans can be encapsulated in it.

Specifically, the AV zone starts from a random single node within the candidate area, and then, as per SAA, is expanded by converting a neighboring non-AV node (i.e., the preceding or succeeding non-AV nodes of AV nodes, see Figure 3-5) within the candidate area to an AV node (we refer to the new AV zone as the "neighboring AV zone") at each iteration. To verify whether the neighboring AV zone is feasible, i.e., being surrounded by a closed cordon, the cutset-based algorithm proposed by Zhang and Yang (2004) can be applied. Specifically, a cutset of a graph is defined as "a minimal collection of links whose removal reduces the rank of the graph by one (and only one)." If the cut that separates the AV zone and non-AV zone is a cutset, then a new feasible design plan is generated; otherwise, another neighboring AV zone will be considered. Doing so leads to a better efficiency of finding new feasible plans, as the probability of a neighboring AV zone being a closed cordon is very high.

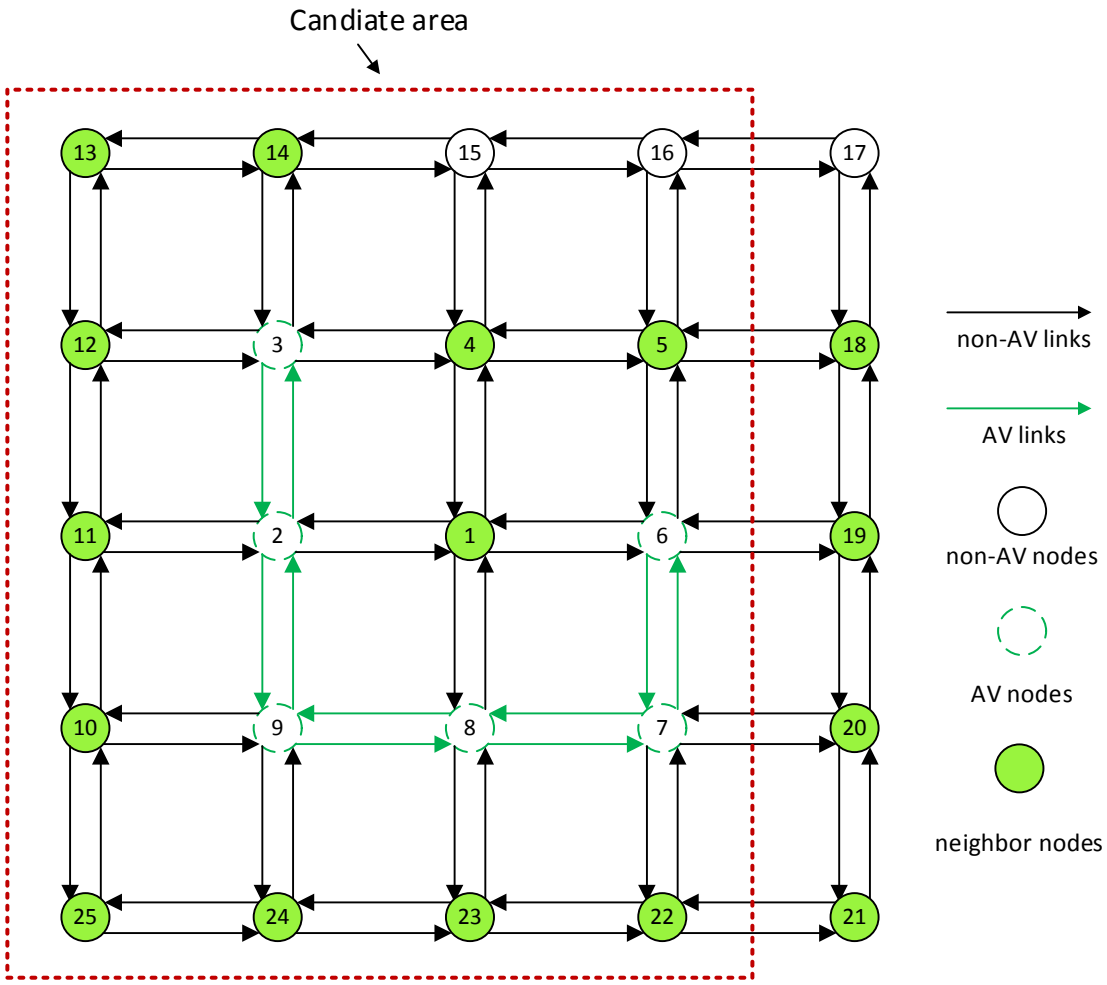

Figure 3-5. A sample AV zone

3.3.2 Numerical Example

In this section, numerical examples are conducted based on a network with 81 nodes and 288 links (see Figure 3-6). The dotted red line illustrates the candidate area where AV nodes can only be located. The Bureau of Public Roads (BPR) function, $t_a = t_a^0\left(1 + 0.15\left(\frac{v_a}{C_a}\right)^4\right)$ is adopted as the link performance function, where t_a^0 and C_a are free-flow travel time and capacity of link a, respectively. Their values are randomly generated from intervals (5, 20) and (5, 100), respectively. In particular, as per Assumption iii, we assume that the per-lane capacity triples when a regular link is converted to an AV link. The O-D demand is displayed in Table 3-9. Without losing generality, we assume that the construction cost for AV zones is 0.

The optimal AV-zone design is shown in Figure 3-6. Observed from the AV zone, interestingly, it is unlike the best tolling cordons found by Zhang and Yang (2004) and Sumalee (2004), which are rounded; instead, it has a relatively long and narrow shape. Such a design can prevent CVs from detouring too much while providing privilege for AVs, as CVs can drive across the AV zone via particular AV nodes (e.g., node 2 and 13; recall that CVs are forbidden to use AV links instead of AV nodes). For example, path $55 \rightarrow 30 \rightarrow 13 \rightarrow 14 \rightarrow 3 \rightarrow 2 \rightarrow 9 \rightarrow 24 \rightarrow 23 \rightarrow 22 \rightarrow 21 \rightarrow 42 \rightarrow 71$ is an available path for CVs from origin 55 to destination 71. Therefore, the AV zone design appears reasonable, as, while reducing the travel cost of AVs, it will not compromise the welfare of CVs too much, and may even improve it.

Table 3-10 shows the travel costs with and without the AV zone deployed. Specifically, with the AV zone deployed, the system travel cost is reduced from 4,169,761 min to 3,278,468 min. That is, the AV zone has reduced the social cost by 21.4%. As mentioned previously, AV-zone planners may be interested in the cost within the AV-zone area. As shown in Table 3-10, the travel cost within the AV-zone area has been reduced by 57.5%. In addition, with the AV zone deployed, the travel cost outside the AV-zone area decreases by 16.8%, although it is not as significant as the one within the AV-zone area. For an additional illustration, Figure 3-7 plots the travel cost saving distribution of CVs. The travel cost savings for all CV trips are positive, which implies that no CV will suffer from the deployment of the AV zone. That is, such a designed AV zone reduces the travel cost of AVs as well as that of CVs, which is in agreement with the discussion in the previous paragraph.

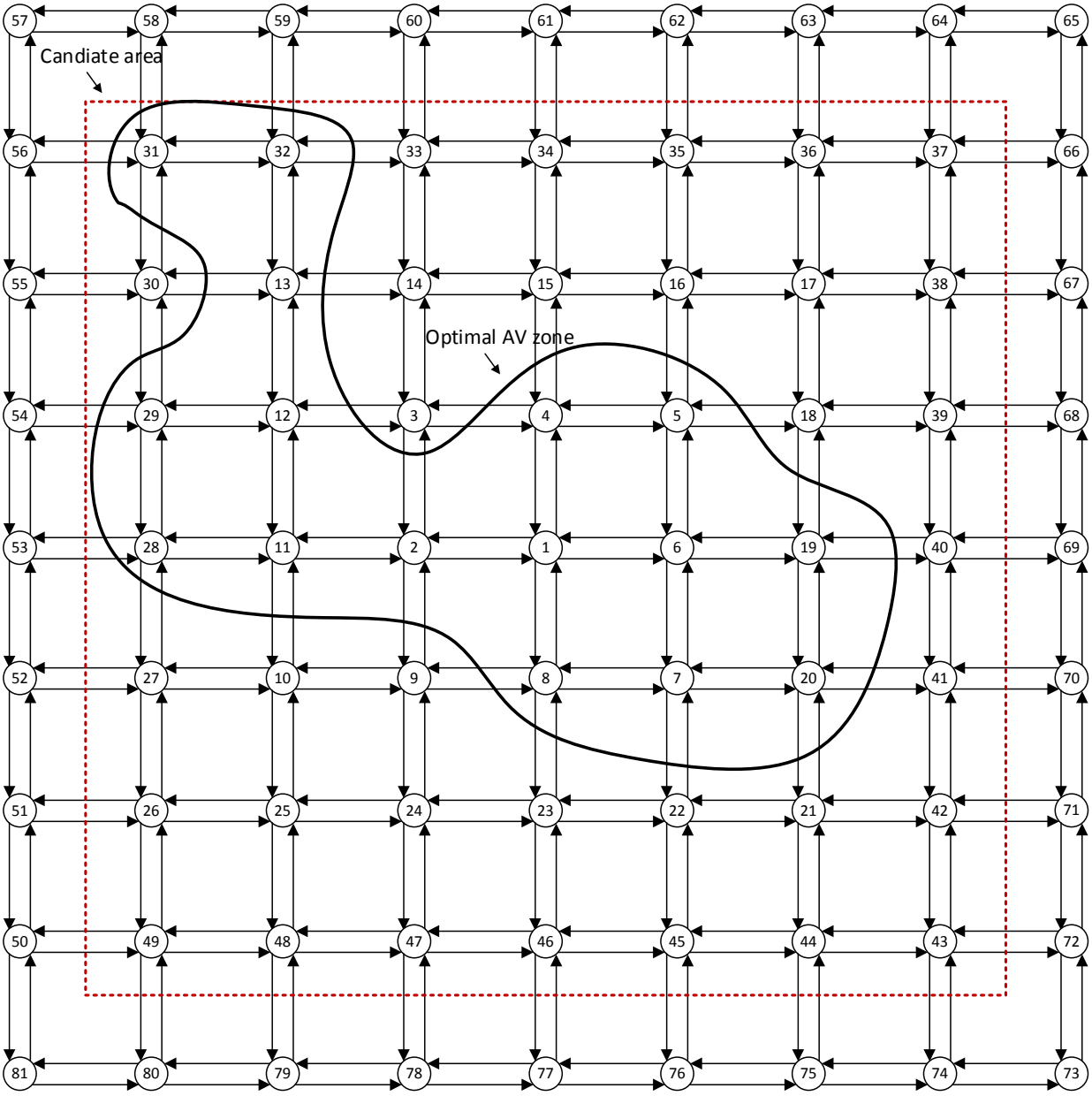

Figure 3-6. Network for the AV zone design

Table 3-9. O-D demand

O-D	CV	AV	O-D	CV	AV	O-D	CV	AV
55-71	20	24	58-73	20	24	72-59	30	36
55-72	30	36	58-74	30	36	73-55	20	24
55-73	40	48	58-75	30	36	73-56	30	36
55-74	20	24	59-71	20	24	73-57	40	48
55-75	20	24	59-72	30	36	73-58	20	24
56-71	30	36	59-73	40	48	73-59	20	24
56-72	20	24	59-74	20	24	74-55	30	36
56-73	20	24	59-75	20	24	74-56	20	24
56-74	30	36	71-55	20	24	74-57	20	24
56-75	30	36	71-56	30	36	74-58	30	36
57-71	20	24	71-57	40	48	74-59	30	36
57-72	30	36	71-58	20	24	75-55	20	24
57-73	40	48	71-59	20	24	75-56	30	36
57-74	20	24	72-55	30	36	75-57	40	48
57-75	20	24	72-56	20	24	75-58	20	24
58-71	30	36	72-57	20	24	75-59	20	24
58-72	20	24	72-58	30	36			

Table 3-10. Travel costs with and without the AV zone

Scenario	System travel cost (min)	Travel cost within the AV-zone area (min)	Travel cost outside of the AV-zone area (min)
Without AV zone	4,169,761	471,755	3,698,005
With AV zone	3,278,468	200,688	3,077,780

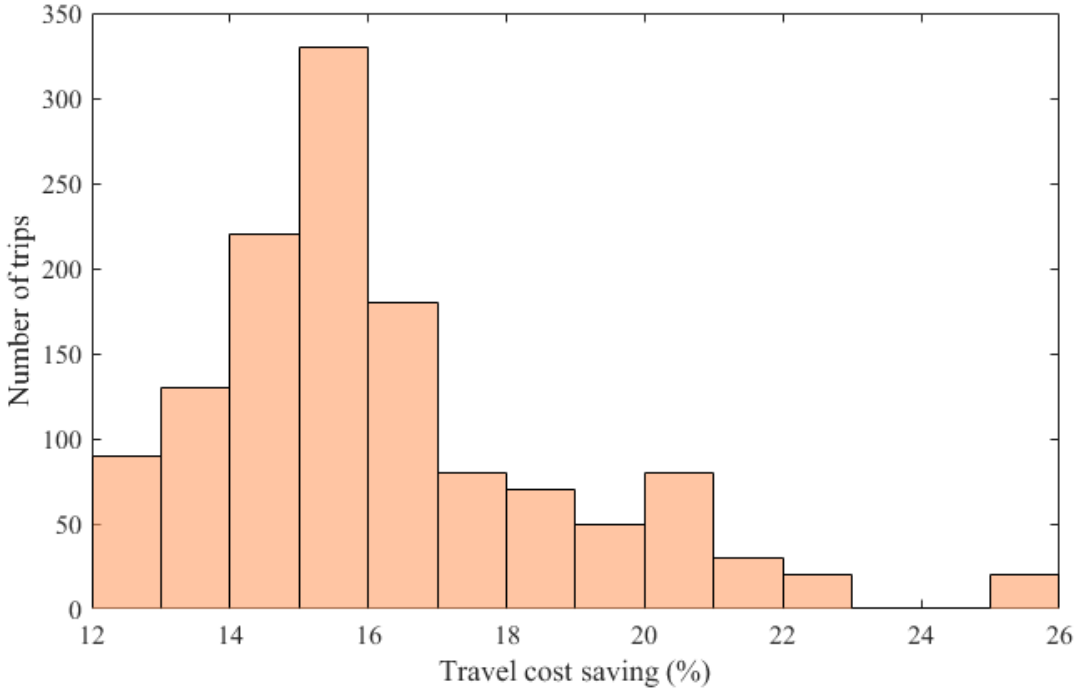

Figure 3-7. Travel cost saving distribution of CVs

CHAPTER 4 CONCLUSION

Envisioning that AVs will be deployed in the future and government agencies can dedicate certain lanes and areas as AV lanes and zones to further promote the adoption of AVs as well as enhance the transportation network performance, this report first proposed a mathematical procedure to optimally deploy AV lanes considering the endogenous AV market penetration. Given AV lanes deployed in a general road network, the flow distributions of both CVs and AVs were captured by a multi-class network equilibrium model. Further, a diffusion model integrating the net benefit derived from deploying AV lanes was applied to forecast the evolution of AV market penetration over time. Based on the network equilibrium model and the diffusion model, a time-dependent deployment model was further formulated to optimize the deployment plan of AV lanes. The deployment plan indicates when, where, and how many AV lanes to be located. The optimization model formulated is a mathematical problem with complementarity constraints, and an efficient active-set algorithm was applied to solve it. Numerical examples were presented to validate the proposed deployment model, and to demonstrate the importance of designing an appropriate deployment plan. Moreover, sensitivity analyses for various critical parameters were conducted. Results show that (1) AV lanes should be deployed following a progressive process instead of a radical one; (2) AV lanes should not be widely deployed until the AV market penetration reaches a relative high level (e.g., more than 20%); (3) lower additional annual cost and VOT for AVs, higher unsafety factor for using CVs, and higher number of annual trips have positive impact on promoting the AV adoption, while the variance of the per-lane capacity of AV lanes has little impact.

Also, this report developed a mathematical framework to optimally design AV zones. To this end, an innovative mixed routing equilibrium model was firstly proposed to describe the flow distribution of CVs and AVs with the presence of AV zones on a road network. Specifically, different from the traditional mixed equilibrium model where each type of player only obeys a particular routing principle across the whole network, AVs apply the user-optimum routing principle when outside of the AV zones, but follow the system-optimum routing principle within the AV zones. This results in a mixed routing behavior for AVs. To capture such a phenomenon, a dummy network was constructed to replace the original AV network where each dummy link represents a set of paths connecting an entrance and an exit of the AV zone; accordingly, the travel cost of each dummy link is in fact the travel cost of the associated entrance and exit pair. As a result, formulating the mixed routing equilibrium model across the original network is equivalent to establishing a traditional network equilibrium model on the revised network. With the established mixed routing equilibrium model, a mixed-integer bi-level programming model was proposed to obtain the optimal design plan of AV zones. The SAA heuristic algorithm was then adopted to solve the model efficiently. Numerical examples show that the social cost may be reduced substantially by an optimal deployment of AV zones.

REFERENCES

Aghassi, M., Bertsimas, D., and Perakis, G., 2006. Solving asymmetric variational inequalities via convex optimization. *Operations Research Letters*, 34, 481-490.

Ban, X. J., Ferris, M., Tang, L., and Lu, S., 2013. Risk-neutral second best toll pricing. *Transportation Research Part B*, 48, 67-87.

Cerny, V., 1985. A thermodynamic approach to the traveling salesman problem: An efficient simulation. *Journal of Optimization Theory and Applications*, 45, 41-51.

Chen, Z., He, F., and Yin, Y., 2016. Optimal deployment of charging lanes in transportation networks. *Transportation Research Part B*, 91, 344-365.

Correia, G. H. d. A., and van Arem, B., 2016. Solving the User Optimum Privately Owned Automated Vehicles Assignment Problem (UO-POAVAP): A model to explore the impacts of self-driving vehicles on urban mobility. *Transportation Research Part B*, 87, 64-88.

de Andrade, G. R., Chen, Z., Elefteriadou, L., and Yin, Y., 2016. Multiclass traffic assignment problem with flow-dependent passenger car equivalent (PCE) value of trucks. *Transportation Research Record* (under review).

Davis, M., 2014. *Integrating autonomous vehicles and managed lanes.* http://www.rsandh.com/blog/2014-06-19-integrating-autonomous-vehicles-and-managed-lanes-2/ (accessed August 18, 2016).

Gao, Z., Wu, J., and Sun, H., 2005. Solution algorithm for the bi-level discrete network design problem. *Transportation Research Part B*, 39, 479-495.

Godsmark, P., and Kakkar, G., 2014. *Why automated vehicle zones make sense*. The Canadian Automated Vehicles Centre of Excellence. https://www.itscanada.ca/files/1_CVAV1_Godsmark_Why%20Automated%20Vehicle%20Zones%20Make%20Sense.pdf (accessed August 18, 2016).

Google Self-Driving Car Project, 2016. https://www.google.com/selfdrivingcar/ (accessed October 30, 2016).

Harker, P. T., 1988. Multiple equilibrium behaviors on networks. *Transportation Science*, 22, 39-46.

Harker, P. T., and Pang, J. S., 1990. Finite-dimensional variational inequality and nonlinear complementarity problems: a survey of theory, algorithms and applications. *Mathematical Programming*, 48, 161-220.

Haurie, A., and Marcotte, P., 1985. On the relationship between Nash-Cournot and Wardrop equilibria. *Networks*, 15, 295-308.

He, F., Wu, D., Yin, Y., and Guan, Y., 2013a. Optimal deployment of public charging stations for plug-in hybrid electric vehicles. *Transportation Research Part B*, 47, 87-101.

He, F., Yin, Y., Shirmohammadi, N., and Y. Nie., 2013b. Tradable credit schemes on networks with mixed equilibrium Behaviors. *Transportation Research Part B*, 57, 47-65.

He, F., Yin, Y., and Zhou, J., 2015. Deploying public charging stations for electric vehicles on urban road networks. *Transportation Research Part C*, 60, 227-240.

Huang, H. J., and Li, Z. C., 2007. A multiclass, multicriteria logit-based traffic equilibrium assignment model under ATIS. *European Journal of Operational Research*, 176(3), 1464-1477.

Hult, E. E., 2006. *Closed charging cordon design problem*. University of Cambridge, UK, 2006.

Kirkpatrick, S., Gelatt, C. D., and Vecchi, M. P., 1983. Optimization by simulated annealing. *Science*, 220, 621-630.

Lavasani, M., Jin, X., and Du, Y., 2016. Market Penetration Model for Autonomous Vehicles Based on Previous Technology Adoption Experiences. In *Transportation Research Board 95th Annual Meeting* (No. 16-2284).

LeBlanc, L.J., 1975. An algorithm for the discrete network design problem. *Transportation Science*, 9, 183-199.

Levin, M., and Boyles, S., 2016a. A multiclass cell transmission model for shared human and autonomous vehicle roads. *Transportation Research Part C*, 62, 103-116.

Levin, M., and Boyles, S., 2016b. A cell transmission model for dynamic lane reversal with autonomous vehicles. *Transportation Research Part C*, 68, 126-143.

Lou, Y., Yin, Y., and Lawphongpanich, S., 2010. Robust congestion pricing under boundedly rational user equilibrium. *Transportation Research Part B*, 44, 15-28.

Luo, Z. Q., Pang, J. S., and Ralph, D., 1996. *Mathematical Programs with Equilibrium Constraints*. Cambridge University Press, New York, New York.

Massiani, J., and Gohs, A., 2015. The choice of Bass model coefficients to forecast diffusion for innovative products: An empirical investigation for new automotive technologies. *Research in Transportation Economics*, *50*, 17-28.

nuTonomy, 2016. http://nutonomy.com/press.html (accessed August 25, 2016).

Park, S. Y., Kim, J. W., and Lee, D. H., 2011. Development of a market penetration forecasting model for Hydrogen Fuel Cell Vehicles considering infrastructure and cost reduction effects. *Journal of Energy Policy*, 39, 3307-3315.

Sumalee, A., 2004. Optimal road user charging cordon design: A heuristic optimization approach. *Computer-Aided Civil and Infrastructure Engineering*, 19, 377-392.

Wang, S., Meng, Q., and Yang, H., 2013. Global optimization methods for the discrete network design problem. *Transportation Research Part B*, 50, 42-60.

Wardrop, J. G., 1952. Some theoretical aspects of road traffic research. *ICE Proceedings: Enginnering Divisions*, 1, 325-362.

Wu, D., Yin, Y., and Lawphongpanich, S., 2011. Pareto-improving congestion pricing on multimodal transportation networks. *European Journal of Operational Research*, 210, 660-669.

Wu, D., Yin, Y., Lawphongpanich, S., and Yang, H., 2012. Design of more equitable congestion pricing and tradable credit schemes for multimodal transportation networks. *Transportation Research Part B*, 46, 1273-1287.

Wu, J. H., Florian, M., and He, S., 2006. An algorithm for multi-class network equilibrium problem in PCE of trucks: application to the SCAG travel demand model. *Transportmetrica*, 2, 1-9.

Yang, H., and Meng, Q., 2001. Modeling user adoption of advanced traveler information systems: dynamic evolution and stationary equilibrium. *Transportation Research Part A*, 35, 895-912.

Yang, H., and Zhang, X., 2008. Existence of anonymous link tolls for system optimum on networks with mixed equilibrium behaviors. *Transportation Research Part B*, 42, 99-112.

Yin, Y., Lawphongpanich, S., and Lou, Y., 2008. Estimating investment requirement for maintaining and improving highway systems. *Transportation Research Part C*, 16, 199-211.

Zhang, L., Lawphongpanich, S., and Yin, Y., 2009. An active-set algorithm for discrete network design problems. *Transportation and Traffic Theory 2009: Golden Jubilee 2009*, 283-300.

Zhang, L., Yang, H., Wu, D., and Wang, D., 2014. Solving a discrete multimodal transportation network design problem. *Transportation Research Part C*, 49, 73-86.

Zhang, X., and Yang, H., 2004. The optimal cordon-based network congestion pricing problem. *Transportation Research Part B*, 38, 517-537.

Zhang, X., Yang, H., Huang, H., 2008. Multiclass multicriteria mixed equilbirum on networks and uniform link tolls for system optimum. *European Journal of Operational Research*, 189, 146-158.

APPENDIX: PROOF OF PROPOSITION 1

This appendix includes the proof of proposition 1. For convenience, we rewrite $\Lambda = \{(\boldsymbol{v}, \boldsymbol{x}, \tilde{\boldsymbol{\rho}}, \boldsymbol{z}, \boldsymbol{\tau})\}$ as follows:

$$\boldsymbol{\Delta x}^{w,m} = \boldsymbol{E}^{w,m}\boldsymbol{d}^{w,m} \qquad \forall m \in M, w \in W \qquad \text{(A.1)}$$

$$v_a = \sum_{w\in W}\sum_{m\in M} x_a^{w,m} \qquad \forall a \in A \cup \hat{A} \qquad \text{(A.2)}$$

$$v_{\tilde{a}} = \sum_{\tilde{w}\in\tilde{W}} x_{\tilde{a}}^{\tilde{w}} \qquad \forall \tilde{a} \in \tilde{A} \qquad \text{(A.3)}$$

$$x_a^{w,A} \geq 0 \qquad \forall a \in A \cup \hat{A}, w \in W \qquad \text{(A.4)}$$

$$x_a^{w,C} \geq 0 \qquad \forall a \in A, w \in W \qquad \text{(A.5)}$$

$$x_a^{w,C} = 0 \qquad \forall a \in \hat{A}, w \in W \qquad \text{(A.6)}$$

$$x_{\tilde{a}}^{\tilde{w}} \geq 0 \qquad \forall \tilde{a} \in \tilde{A}, \tilde{w} \in \tilde{W} \qquad \text{(A.7)}$$

$$\tilde{\rho}_i^{\tilde{w}} \geq 0 \qquad \forall i \in \tilde{N}, \tilde{w} \in \tilde{W} \qquad \text{(A.8)}$$

$$\tau_i^{\tilde{w}} \geq 0 \qquad \forall i \in \tilde{N}\backslash d(\tilde{w}), \tilde{w} \in \tilde{W} \qquad \text{(A.9)}$$

$$\tilde{\Delta}\boldsymbol{z}^{\tilde{w}} = \tilde{E}^{\tilde{w}} \qquad \forall \tilde{w} \in \tilde{W} \qquad \text{(A.10)}$$

$$z_{\tilde{a}}^{\tilde{w}} \geq 0 \qquad \forall \tilde{a} \in \tilde{A}, \tilde{w} \in \tilde{W} \qquad \text{(A.11)}$$

The optimality conditions of MRE-VI can be stated as follows:

(A.1)-(A.11)

$$t_a(v_a) - \gamma_a = 0 \qquad \forall a \in A \qquad \text{(A.12)}$$

$$\sum_{\tilde{w}\in\tilde{W}} \beta_a^{\tilde{w}} \sum_{\tilde{a}\in\tilde{A}} t_{\tilde{a}}(v_{\tilde{a}}) z_{\tilde{a}}^{\tilde{w}} - \gamma_a = 0 \qquad \forall a \in \hat{A} \qquad \text{(A.13)}$$

$$-\gamma_{\tilde{a}} = 0 \qquad \forall \tilde{a} \in \tilde{A} \qquad \text{(A.14)}$$

$$-\rho_i^{w,m} + \rho_j^{w,m} + \gamma_a - \xi_a^{w,m} = 0 \qquad \forall a \in A \cup \hat{A}, m \in M, w \in W \qquad \text{(A.15)}$$

$$t_{\tilde{a}}(v_{\tilde{a}}) + v_{\tilde{a}} t'_{\tilde{a}}(v_{\tilde{a}}) - \tilde{\rho}_i^{\tilde{w}} + \tilde{\rho}_j^{\tilde{w}} + \gamma_{\tilde{a}} - \mu_{\tilde{a}}^{\tilde{w}} = 0 \qquad \forall \tilde{a} = (i,j), \tilde{w} \in \tilde{W} \qquad \text{(A.16)}$$

$$\left(\sum_j x_{o(\tilde{w}),j}^{\tilde{w}} - \sum_k x_{k,o(\tilde{w})}^{\tilde{w}}\right) - \sum_{a\in\hat{A}} \beta_a^{\tilde{w}} \sum_{w\in W} x_a^{w,A} - \theta_{o(\tilde{w})}^{\tilde{w}} = 0 \qquad \forall \tilde{w} \in \tilde{W} \qquad \text{(A.17)}$$

$$-\left(\sum_j x_{o(\tilde{w}),j}^{\tilde{w}} - \sum_k x_{k,o(\tilde{w})}^{\tilde{w}}\right) + \sum_{a\in\hat{A}} \beta_a^{\tilde{w}} \sum_{w\in W} x_a^{w,A} - \varsigma_{o(\tilde{w})}^{\tilde{w}} = 0 \qquad \forall \tilde{w} \in \tilde{W} \qquad \text{(A.18)}$$

$$\left(\sum_j x_{i,j}^{\tilde{w}} - \sum_k x_{k,i}^{\tilde{w}}\right) - \theta_i^{\tilde{w}} = 0 \qquad \forall i \in \tilde{N}\backslash\{o(\tilde{w}), d(\tilde{w})\}, \tilde{w} \in \tilde{W} \qquad \text{(A.19)}$$

$$\left(\sum_j x_{i,j}^{\tilde{w}} - \sum_k x_{k,i}^{\tilde{w}}\right) - \varsigma_i^{\tilde{w}} = 0 \qquad \forall i \in \tilde{N}\backslash\{o(\tilde{w}), d(\tilde{w})\}, \tilde{w} \in \tilde{W} \qquad \text{(A.20)}$$

$$t_{\tilde{a}}(v_{\tilde{a}}) - \kappa_i^{\tilde{w}} + \kappa_j^{\tilde{w}} - \alpha_{\tilde{a}}^{\tilde{w}} = 0 \qquad \forall \tilde{a} \in \tilde{A}, \tilde{w} \in \tilde{W} \qquad \text{(A.21)}$$

$$x_a^{w,A}\xi_a^{w,A} = 0 \qquad \forall a \in A \cup \hat{A}, w \in W \qquad \text{(A.22)}$$

$$x_a^{w,C}\xi_a^{w,C} = 0 \qquad \forall a \in A, w \in W \qquad \text{(A.23)}$$

$$x_{\tilde{a}}^{\tilde{w}}\mu_{\tilde{a}}^{\tilde{w}} = 0 \qquad \forall \tilde{a} \in \tilde{A}, \tilde{w} \in \tilde{W} \qquad \text{(A.24)}$$

$$\tilde{\rho}_i^{\tilde{w}}\theta_i^{\tilde{w}} = 0 \qquad \forall i \in \tilde{N}, \tilde{w} \in \tilde{W} \qquad \text{(A.25)}$$

$$\tau_i^{\tilde{w}} \varsigma_i^{\tilde{w}} = 0 \qquad \forall i \in \tilde{N} \backslash d(\tilde{w}),\ \tilde{w} \in \tilde{W} \qquad \text{(A.26)}$$

$$z_{\tilde{a}}^{\tilde{w}} \alpha_{\tilde{a}}^{\tilde{w}} = 0 \qquad \forall \tilde{a} \in \tilde{A}, \tilde{w} \in \tilde{W} \qquad \text{(A.27)}$$

$$\xi_a^{w,A} \geq 0 \qquad \forall a \in A \cup \hat{A}, w \in W \qquad \text{(A.28)}$$

$$\xi_a^{w,C} \geq 0 \qquad \forall a \in A, w \in W \qquad \text{(A.29)}$$

$$\mu_{\tilde{a}}^{\tilde{w}} \geq 0 \qquad \forall \tilde{a} \in \tilde{A}, \tilde{w} \in \tilde{W} \qquad \text{(A.30)}$$

$$\theta_i^{\tilde{w}} \geq 0 \qquad \forall \tilde{w} \in \tilde{W} \qquad \text{(A.31)}$$

$$\varsigma_i^{\tilde{w}} \geq 0 \qquad \forall i \in \tilde{N} \backslash d(\tilde{w}),\ \tilde{w} \in \tilde{W} \qquad \text{(A.32)}$$

$$\alpha_{\tilde{a}}^{\tilde{w}} \geq 0 \qquad \forall \tilde{a} \in \tilde{A}, \tilde{w} \in \tilde{W} \qquad \text{(A.33)}$$

where $\rho_i^{w,m}$, γ_a, $\gamma_{\tilde{a}}$, $\xi_a^{w,A}$, $\mu_{\tilde{a}}^{\tilde{w}}$, $\theta_i^{\tilde{w}}$, $\varsigma_i^{\tilde{w}}$, $\kappa_i^{\tilde{w}}$, and $\alpha_{\tilde{a}}^{\tilde{w}}$ are the multipliers of constraints (A.1)-(A.4), and (A.7)-(A.11); $\xi_a^{w,C}$ is the multiplier of constraints (A.5) and (A.6).

From (A.12), (A.15), and (A.22), we have:

$$\left[t_a(v_a) - \rho_i^{w,A} + \rho_j^{w,A}\right] x_a^{w,A} = 0, \forall a \in A, w \in W \qquad \text{(A.34)}$$

From (A.12), (A.15), and (A.28), we have:

$$t_a(v_a) - \rho_i^{w,A} + \rho_j^{w,A} \geq 0, \forall a \in A, w \in W \qquad \text{(A.35)}$$

From (A.12), (A.15), and (A.23), we have:

$$\left[t_a(v_a) - \rho_i^{w,C} + \rho_j^{w,C}\right] x_a^{w,C} = 0, \forall a \in A, w \in W \qquad \text{(A.36)}$$

From (A.12), (A.15), and (A.29), we have:

$$t_a(v_a) - \rho_i^{w,C} + \rho_j^{w,C} \geq 0, \forall a \in A, w \in W \qquad \text{(A.37)}$$

From (A.13), (A.15), and (A.22), we have:

$$\left[\sum_{\tilde{w} \in \tilde{W}} \beta_a^{\tilde{w}} \sum_{a \in A} t_{\tilde{a}}(v_{\tilde{a}}) z_{\tilde{a}}^{\tilde{w}} - \rho_i^{w,A} + \rho_j^{w,A}\right] x_a^{w,A} = 0, \forall a \in \hat{A}, w \in W \qquad \text{(A.38)}$$

From (A.13), (A.15), and (A.28), we have:

$$\sum_{\tilde{w} \in \tilde{W}} \beta_a^{\tilde{w}} \sum_{a \in A} t_{\tilde{a}}(v_{\tilde{a}}) z_{\tilde{a}}^{\tilde{w}} - \rho_i^{w,A} + \rho_j^{w,A} \geq 0, \forall a \in \hat{A}, w \in W \qquad \text{(A.39)}$$

From (A.14), (A.16), and (A.24), we have:

$$\left[t_{\tilde{a}}(v_{\tilde{a}}) + v_{\tilde{a}} t'_{\tilde{a}}(v_{\tilde{a}}) - \tilde{\rho}_i^{\tilde{w}} + \tilde{\rho}_j^{\tilde{w}}\right] x_{\tilde{a}}^{\tilde{w}} = 0, \forall \tilde{a} = (i,j) \in \tilde{A}, \tilde{w} \in \tilde{W} \qquad \text{(A.40)}$$

From (A.14), (A.16), and (A.30), we have:

$$t_{\tilde{a}}(v_{\tilde{a}}) + v_{\tilde{a}} t'_{\tilde{a}}(v_{\tilde{a}}) - \tilde{\rho}_i^{\tilde{w}} + \tilde{\rho}_j^{\tilde{w}} \geq 0, \forall \tilde{a} = (i,j) \in \tilde{A}, \tilde{w} \in \tilde{W} \qquad \text{(A.41)}$$

From (A.17) and (A.31), we have:

$$\left(\sum_j x^{\tilde{w}}_{o(\tilde{w}),j} - \sum_k x^{\tilde{w}}_{k,o(\tilde{w})}\right) - \sum_{a\in\hat{A}} \beta^{\tilde{w}}_a \sum_{w\in W} x^{w,A}_a = \theta^{\tilde{w}}_{o(\tilde{w})} \geq 0, \forall \tilde{w} \in \tilde{W} \quad \text{(A.42)}$$

From (A.18) and (A.32), we have:

$$-\left(\sum_j x^{\tilde{w}}_{o(\tilde{w}),j} - \sum_k x^{\tilde{w}}_{k,o(\tilde{w})}\right) + \sum_{a\in\hat{A}} \beta^{\tilde{w}}_a \sum_{w\in W} x^{w,A}_a = \varsigma^{\tilde{w}}_{o(\tilde{w})} \geq 0, \forall \tilde{w} \in \tilde{W} \quad \text{(A.43)}$$

We know that (A.42) and (A.43) can hold only if $\theta^{\tilde{w}}_{o(\tilde{w})} = 0, \varsigma^{\tilde{w}}_{o(\tilde{w})} = 0, \forall \tilde{w} \in \tilde{W}$ and

$$\left(\sum_j x^{\tilde{w}}_{o(\tilde{w}),j} - \sum_k x^{\tilde{w}}_{k,o(\tilde{w})}\right) = \sum_{a\in\hat{A}} \beta^{\tilde{w}}_a \sum_{w\in W} x^{w,A}_a = 0, \forall \tilde{w} \in \tilde{W} \quad \text{(A.44)}$$

From (A.19) and (A.31), we have:

$$\left(\sum_j x^{\tilde{w}}_{i,j} - \sum_k x^{\tilde{w}}_{k,i}\right) = \theta^{\tilde{w}}_i \geq 0, \forall i \in \tilde{N}\backslash\{o(\tilde{w}), d(\tilde{w})\}, \tilde{w} \in \tilde{W} \quad \text{(A.45)}$$

From (A.20) and (A.32), we have:

$$\left(\sum_j x^{\tilde{w}}_{i,j} - \sum_k x^{\tilde{w}}_{k,i}\right) = \theta^{\tilde{w}}_i \geq 0, \forall i \in \tilde{N}\backslash\{o(\tilde{w}), d(\tilde{w})\}, \tilde{w} \in \tilde{W} \quad \text{(A.46)}$$

Similarly, (A.45) and (A.46) can hold only if: $\theta^{\tilde{w}}_i = 0, \varsigma^{\tilde{w}}_i = 0, \forall \in \tilde{N}\backslash\{o(\tilde{w}), d(\tilde{w})\}, \tilde{w} \in \tilde{W}$ and

$$\sum_j x^{\tilde{w}}_{i,j} - \sum_k x^{\tilde{w}}_{k,i} = 0, \forall i \in \tilde{N}\backslash\{o(\tilde{w}), d(\tilde{w})\}, \tilde{w} \in \tilde{W} \quad \text{(A.47)}$$

Further, summating (A.44) and (A.47), we can obtain:

$$\sum_j x^{\tilde{w}}_{d(\tilde{w}),j} - \sum_k x^{\tilde{w}}_{k,d(\tilde{w})} = -\sum_{a\in\hat{A}} \beta^{\tilde{w}}_a \sum_{w\in W} x^{w,A}_a \quad \text{(A.48)}$$

From (A.21) and (A.27), we have:

$$[t_{\tilde{a}}(v_{\tilde{a}}) - \kappa^{\tilde{w}}_i + \kappa^{\tilde{w}}_j] z^{\tilde{w}}_{\tilde{a}} = 0 \quad \text{(A.49)}$$

From (A.21) and (A.33), we have:

$$t_{\tilde{a}}(v_{\tilde{a}}) - \kappa^{\tilde{w}}_i + \kappa^{\tilde{w}}_j \geq 0 \quad \text{(A.50)}$$

Obviously, (A.1)-(A.11), (A.34)-(A.41), (A.44), and (A.47)-(A.50) are equivalent to the MRE conditions (3-1)-(3-21).

Note that the optimality condition of MRE-VI contains additional constraints, such as, (A.8), (A.9), (A.25), and (A.26), but this will not affect the equivalence.